Molecular Weight Distribution Modeling of Radical Polymerization in a CSTR with Long Chain Branching through Transfer to Polymer and Terminal Double Bond (TDB) Propagation

Piet D. Iedema,* Snezana Grcev, and Huub C. J. Hoefsloot

Department of Chemical Engineering, University of Amsterdam, Nieuwe Achtergracht 166, 1018 WV Amsterdam, The Netherlands

Received June 10, 2002; Revised Manuscript Received October 21, 2002

ABSTRACT: The modeling of free radical polymerization with long chain branching in a CSTR is addressed. Long branches are assumed to be created by transfer to polymer and by insertion of active terminal double bonds (TDBs). Such TDBs may be produced by transfer to monomer and termination by disproportionation. The modeling approach is based on population balances being solved using a Galerkin finite element method (FEM). Two different models have been derived. The "TDB classes" model employs different equations for each class of chains with a certain number of TDBs. The "TDB moment distribution" uses the pseudodistribution method developed by us before[22] for simultaneous molecular weight/degree of branching distribution modeling. Model calculations have been performed for the case of poly(vinyl acetate) (PVAc). In the case of the maximum one TDB per chain, the two models prove to be mathematically equivalent. An increase of TDB propagation rate leads to a broadening of chain length distribution (CLD) and sometimes to a more pronounced "shoulder" at long chain lengths. The significant concentration range extends to extremely long chain lengths (10^{10})—well within a gel regime—but the model could fully cover this. Quite remarkably, concentrations of living chains are higher than those of dead chains in this region. The average number of TDBs per chain could be calculated and turns out to be constant at shorter chain lengths, but becomes lower for longer chains. This is explained by the combined action of chain growth by TDB propagation, which implies TDB consumption as well, and transfer to polymer. For the case of more than one TDB per chain, the two models yield different results depending on closure relationships. The TDB moment distribution model revealed that the longest chains carry tens of thousands of TDBs. The classes model strongly underestimates the number of TDBs and hence the reactivity of the dead chains to TDB propagation. The results show the effect of dead chains with many TDBs acting as cross-linkers for living chains. As an interesting trend, it was observed that with increasing TDB propagation rate an increasing fraction of monomer units existing in polymer chains is present in fewer, but extremely long living, chains.

Introduction

Radical polymerization with long chain branching has been of interest to many authors before due to its relevance to the production of many industrially important polymers like low-density polyethylene, poly(vinyl acetate), and polyacrylates.[1−23] The interest originates from several factors, among which are the excessive broadening of the molecular weight distribution (MWD) encountered eventually leading to gel formation[1,2] and the branchedness of the resulting polymer. The latter leads to highly interesting rheological properties like "strain hardening" [3] and has been considered as an issue for characterization due to the impact of branching on the radius of gyration.[4,5] The most dominant mechanism of long branch formation in radical polymerization considered is transfer to polymer, which by itself can potentially be responsible for a huge broadening of the molecular weight distribution. A second important mechanism leading to long branches is the insertion in propagating living chains of dead chains with terminal double bonds, being created by transfer to monomer or disproportionation termination. This terminal double bond (TDB) propagation has been mainly addressed in the context of PVAc studies[6−19] and somewhat less in ldPE work.[21]

In the present modeling study, we will focus on the impact of the *combination* of the two branching mechanisms, transfer to polymer and terminal double bond propagation, on the MWD. Our approach is the first attempt ever to solve this problem with population balance modeling using the Galerkin finite element method as implemented in the PREDICI package.[24] In addition, we developed a number of new features, so that we now dispose of a general framework applicable to cases with an unlimited number of terminal double bonds and allows simultaneously computing concentration distributions of molecular weight (MWD), degree of branching (DBD), and terminal double bonds (TDBD). The impact of combined transfer to polymer and TDB propagation on MWD has been dealt with before, but with different modeling approaches, Monte Carlo sampling,[6−10] and other methods.[1,11−13]

In our work, the mechanisms selected are in a broad range and in line with the most recent experimental findings as will be put forward next. We excluded chain scission from the analysis, since this topic has been treated in the context of ldPE before.[22] A common aspect of the present study with the ldPE work mentioned, however, is the practical usefulness of MWD calculations with respect to the identification of kinetic mechanisms. When the MWD shape is sensitive to the mechanisms discussed, which was very clearly the case in the ldPE study, then information about the relevance of these mechanisms can be obtained by comparing calculated MWD to accurate measurements of the MWD. We will adopt initiation and propagation as self-evident. In the case of PVAc, the tacticity issue has been raised,[19] but this is of no importance to MWD. Termination through recombination is excluded on the basis of most PVAc studies but is regarded to be important in

10.1021/ma020900v CCC: $25.00
Published on Web 12/17/2002

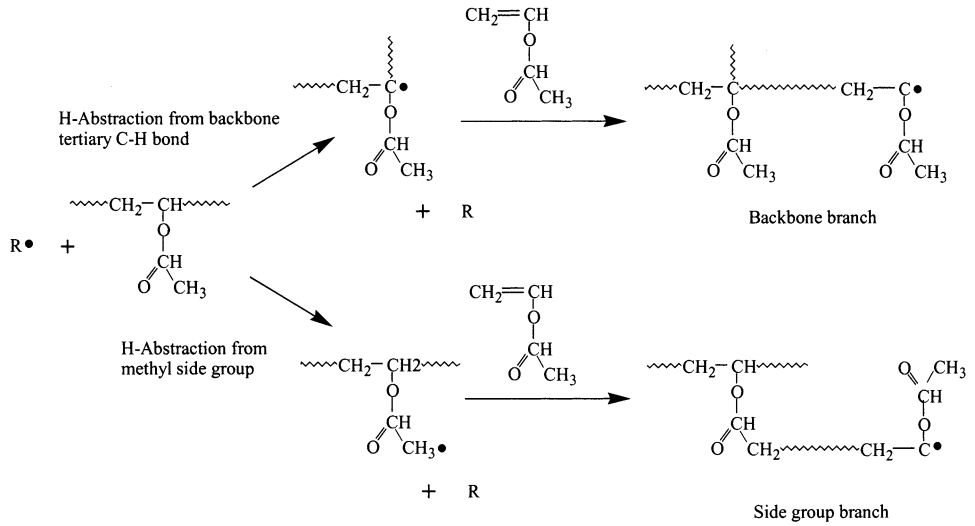

Figure 1. Formation of two types of long branches by transfer to polymer.

ldPE. Disproportionation has been the most commonly accepted termination mechanism for PVAc,[18] but still some authors doubt about its existence.[19] In our simulations, both termination mechanisms will be addressed.

Many authors have investigated transfer to polymer as one of the LCB forming mechanisms in ldPE, PVAc, and PA. Among these is an NMR-based study of PVAc,[19] revealing that branches mainly become attached to the methyl group rather than a backbone C atom (Figure 1). This explains why hydrolyzing PVAc to poly(vinyl alcohol) (PVA) leads to chain length reduction. The other branch-forming mechanism, terminal double bond propagation, has been mainly discussed in the context of PVAc and, in one case, for ldPE.[21] The importance of either or both of the branching mechanisms for gelation has been discussed before. It is argued that these mechanisms in themselves never are able to create gel formation without termination by recombination.[1,6−11] However, on the basis of population balance modeling of the MWD until a cutoff limit, for a system with transfer to polymer only, we found that even without recombination a very long MW tail exists, and hence, gelation is expected. In this publication, we will revisit this topic. In yet another aspect, both branching mechanisms are interesting, since both are capable of producing macromolecules with multiple radical positions.[9] Transfer to polymer takes place to both dead and living chains, but the latter is usually neglected in view of the low living chain concentration. However, it has been argued that transfer to polymer only in the case of a CSTR can lead to conditions under which multiradicals have to be taken into account.[9] We will show that multiradicals may become important not only for transfer to polymer but also for TDB propagation, since one easily may see that apart from dead chains also *living* chains with TDB's may be inserted in a growing chain. Whether or not to take multiradicals into account merely depends on the concentration ratio between living and dead chains, which we will show drastically to increase at long chain length. However, dealing with multiradicals will not be treated in this paper but in a future one especially devoted to this topic.

The last mechanistic issue is concerned with the manner in which *active* terminal double bonds are created in PVAc.[14−16] Most commonly accepted is transfer to monomer as shown in Figure 2 producing a monoradical with a TDB. Subsequent propagation of

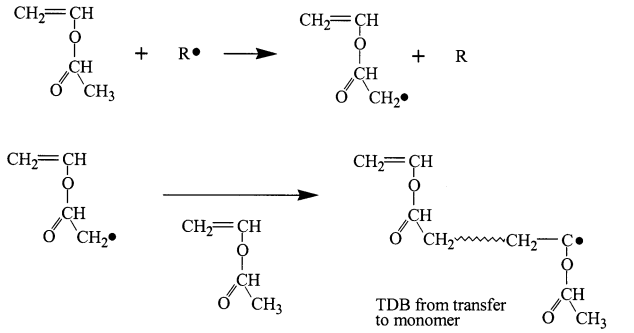

Figure 2. Formation of terminal double bonds by transfer to monomer.

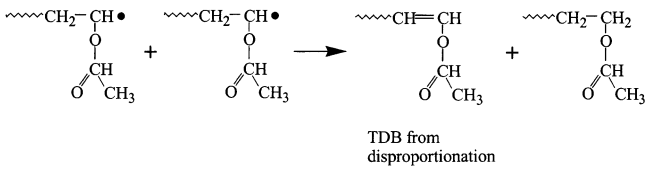

Figure 3. Formation of terminal double bonds by disproportionation.

this monoradical leads to a chain with an active terminal double bond being linked to the chain by an ester linkage. When such a TDB chain is inserted in another growing chain, a branch is created being connected to the growing chain through a hydrolizable bond—it is broken upon hydrolysis and conversion to poly(vinyl alcohol). In this respect, it is indistinguishable from the long branches created at methyl side groups by the transfer to polymer mechanism (Figure 1), which has been shown to be the dominant transfer to polymer process.[19] The second TDB producing mechanism is disproportionation as depicted in Figure 3. TDB propagation of such a chain leads to a long branch being attached in the same way to the growing chain as the branches formed by transfer to the backbone mechanism (Figure 1). These branches cannot be hydrolyzed and will not lead to degradation upon conversion to PVA. In the aforementioned NMR study,[19] no olefinic peaks are found, which is explained, according to this author, by the fast insertion of the 1,1-substituted double bonds resulting from transfer to monomer (Figure 2) and the presumed absence of disproportionation termination. The argument for the latter is linked to the reactivity of the TDB resulting from disproportionation, which is

Table 1. Reactions[a]

initiator dissociation	$I_2 \xrightarrow{k_d} 2I$
initiation	$I + M \xrightarrow{k_i} R_{1,0,0}$
propagation	$R_{n,i,k} + M \xrightarrow{k_p} R_{n+1,i,k}$
termination by disproportionation (without TDB creation)	$R_{n,i,k} + R_{m,j,l} \xrightarrow{k_{td}} P_{n,i,k} + P_{m,j,l}$
termination by disproportionation (with TDB creation)	$R_{n,i,k} + R_{m,j,l} \xrightarrow{k_{td}} P_{n,i+1,k} + P_{m,j,l}$
termination by recombination	$R_{n,i,k} + R_{m,j,l} \xrightarrow{k_{tc}} P_{n+m,i+j,k+l}$
transfer to monomer	$R_{n,i,k} + M \xrightarrow{k_m} P_{n,i,k} + R_{1,1,0}$
transfer to polymer	$R_{n,i,k} + P_{m,j,l} \xrightarrow{k_{tp}m} P_{n,i,k} + R_{m,j,l+1}$
terminal double bond propagation	$R_{n,i,k} + P_{m,j,l} \xrightarrow{k_{db}j} R_{n+m,i+j-1,k+l+1}$

[a] In this article disproportionation is assumed to take place without TDB creation. I_2, I, and M denote concentrations of initiator, initiator radicals and monomers, respectively. Key: m, n, chain length; i, j, number of terminal double bonds (TDB) per chain; k, l, number of branches per chain.

considered to be low since it is a 1,2-substituted double bond. However, an experimental study[18] has shown that the disproportionation mechanism is essential in explaining the found MW data. For this reason, we do not, in principle, exclude disproportionation as termination and active TDB generating mechanism in our simulations. As will be demonstrated, this has a crucial impact on the question whether chains may contain more than one TDB. Most previous studies,[6−13] except one,[1] have assumed one TDB per chain at a maximum. In the present paper, we derive two models for the general case of an arbitrary number of TDBs per chain but then first apply it to the one TDB per chain case. In the case of an arbitrary number of TDBs case, we will see that the existence of multiple TDB chains acting as "cross-linkers" (similar to multiradicals) has a strong impact on the gelation behavior. Note that besides termination by disproportionation also the other termination mechanism, recombination, leads to multiple TDB chains, albeit in quite another way, since it simply allows macroradicals with one or more TDB's to couple.

The structure of this paper is as follows. We start with the reaction equations being addressed in the study accompanied by the 3-dimensional population balance equations, dimensions being formed by chain length, number of TDB's, and number of branches. Next, the simplification to a 2-dimensional problem—not explicitly taking the number of branches distribution into account—is discussed and the proper 2-D population balance equations are derived. We then present two modeling approaches. One employs explicit distribution variables for classes of chains with the same number of TDBs (like it has been performed for branching[21]). The other approach follows earlier work using pseudodistributions.[22] These two models are derived for the general case of an arbitrary number of TDBs per chain. Subsequently, we reduce both models to describe the case of one TDB per chain at maximum and then see that they become equivalent. Finally, simulations for both cases—one and more TDBs per chain—will be discussed and compared, and results will be presented for a model case based on PVAc kinetics, including some variations. This is to demonstrate the effect of termination, transfer to polymer, and TDB propagation constants as well as conversion on chain length and TDB fraction distribution. Special attention will be given to (bimodal) chain length distributions obtained in the gel regime and to the concentration of macroradicals, which responds to earlier discussions on multiradicals.

Model Construction

Problem Formulation. A model is constructed for the kinetic set in Table 1, giving the reaction equations in all three concentration distribution variables: chain length, number of TDB, number of branches. Mathematically we will henceforth denote this as a problem in 3 "dimensions" . Note that we exclude living chains from both transfer and TDB propagation reactions. Most of the equations in the table are self-evident, except the TDB propagation reaction that deserves closer examination, not in the least since it leads to one of the central modeling problems to be solved in this work. The reaction equation reads

$$R_{n,i,k} + P_{m,j,l} \xrightarrow{k_{db}j} R_{n+m,i+j-1,k+l+1} \qquad (1)$$

In fact, this represents a combination reaction that sums up chain lengths, while numbers of branches are summed up along with the addition of one extra branch created by the reaction, while TDB's are summed up as well except for one TDB consumed in the reaction. Evidently, the reactivity of the dead chain inserted is proportional to the number of TDB's it carries. As such, this is similar to the transfer to polymer reaction, where the reactivity is proportional to the number of monomer units in the chain. Since the latter mechanism introduces a nonlinearity in the mathematical modeling of the system, it is often denoted as "nonlinear" polymerization. In 1-dimensional chain length modeling using the population balance equations and solving them with the Galerkin FEM scheme, the chain length is already explicitly present in the equations, which renders their solution to a fairly easy operation. Similarly, TDB propagation introduces another nonlinearity, but in contrast, in a simple, 1-dimensional chain length model the number of TDBs is not counted, since it is not an explicit variable. Mathematically speaking, to solve the problem in one dimension, chain length, one has to solve it in the second dimension, TDB number, as well. How

Table 2. Full 3-Dimensional Set of Population Balance Equations in Living and Dead Chain Concentration Variables $R_{n,i,k}$ and $P_{n,i,k}$[a]

initiator dissociation	$\frac{dI_2}{dt} = -k_d I_2 - \frac{I_2}{\tau}$
initiation	$\frac{dI}{dt} = 2k_d I_2 - k_i MI - \frac{I}{\tau}; \frac{dR_{1,0,0}}{dt} += k_i MI$
propagation	$\frac{dR_{n,i,k}}{dt} += k_p M(R_{n-1,i,k} - R_{n,i,k})$
termination by disproportionation (TDB creation)	$\frac{dR_{n,i,k}}{dt} += -k_{td}\lambda_0 R_{n,i,k}; \quad \frac{dP_{n,i,k}}{dt} += \frac{1}{2}k_{td}\lambda_0(R_{n,i-1,k} + R_{n,i,k})^b$
termination by recombination	$\frac{dR_{n,i,k}}{dt} += -k_{tc}\lambda_0 R_{n,i,k}; \quad \frac{dP_{n,i,k}}{dt} += \frac{1}{2}k_{tc}\sum_{m=1}^{n-1}\sum_{j=0}^{i}\sum_{l=0}^{k} R_{m,j,l}R_{n-m,i-j,k-l}$
transfer to monomer	$\frac{dR_{n,i,k}}{dt} += -k_m MR_{n,i,k}; \quad \frac{dR_{1,1,0}}{dt} += k_m\lambda_0 M$
	$\frac{dP_{n,i,k}}{dt} += k_m MR_{n,i,k}$
transfer to polymer	$\frac{dR_{n,i,k}}{dt} += k_{tp}(\lambda_0 nP_{n,i,k-1} - \mu_1 R_{n,i,k})$
	$\frac{dP_{n,i,k}}{dt} += k_{tp}(-\lambda_0 nP_{n,i,k} + \mu_1 R_{n,i,k})$
terminal double bond propagation	$\frac{dR_{n,i,k}}{dt} += k_{db}(-R_{n,i,k}\sum_{n=1}^{\infty}\sum_{i=0}^{\infty}\sum_{k=0}^{\infty} iP_{n,i,k} + \sum_{m=1}^{n-1}\sum_{j=0}^{i+1}\sum_{l=0}^{k} jP_{m,j,l}R_{n-m,i-j+1,k-l-1})$
	$\frac{dP_{n,i,k}}{dt} += -k_{db} i\lambda_0 P_{n,i,k}$

[a] For indices, see Table 1. Summation over the branching index k yielding a 2-D formulation of exactly the same form provides the basis for the TDB classes model. In the classes, model 2-D variables $R_{n,i}$ and $P_{n,i}$ are replaced by 1-D variables for chains with specific numbers of TDBs, ${}^iR_n$ and ${}^iP_n$. The $+=$ duet means a contribution to the overall balance equation of the respective species. [b] The first term in parentheses equals zero in the case where TDB creation by disproportionation is not accounted for.

to deal with the TDB-dependent reactivity is one of the essential modeling problems of this work. We present two different approaches to solve it. The first one employs different distribution variables for living and dead chains with 0, 1, 2, 3, etc. TDB's, which is called "TDB classes modeling" , cf. "branching classes modeling".[21] The other is "TDB moment modeling" utilizing the pseudodistribution method introduced in our earlier MWD/DBD work.[22]

The fundamental difference between 2-dimensional molecular weight and branching distribution modeling and 2-D TDB/MW distribution modeling should be stressed once more. In the MW/DB distribution case, the only impact of the branching distribution on the kinetics proceeds through the chain scission reaction, as has been demonstrated clearly before.[22] Hence, not including scission implies that finding the DBD simply is an "add-on" to MWD-modeling—DBD does not have any feedback on MWD. In the present 2-D distribution modeling problem of MW and TDB, such a feedback is definitely present. The fact that the MW/TDB distribution is independent of branching is convenient, since it in principle allows us to treat branching as a separate issue.

The full 3-D molecular weight-terminal double bond-branching population balance equations belonging to the reactions as given in Table 1 are listed in Table 2. Note that this system is an exact representation of the reactions in Table 1, no assumptions have yet been made, and it is valid for cases with an arbitrary number of TDBs per chain. In the present case of a CSTR, the complete population balances of all distributions Q_n contain an outflow term of the general shape Q_n/τ, where τ represents the average residence time (equal to volume/volumetric flow). The overall moments λ_0 and μ_1 are defined as usual, and in the 3-D case, they follow as

$$\lambda_0 = \sum_{i=0}^{\infty}\sum_{k=0}^{\infty}\sum_{n=1}^{\infty} R_{n,i,k}\ \mu_1 = \sum_{i=0}^{\infty}\sum_{k=0}^{\infty}\sum_{n=1}^{\infty} nP_{n,i,k} \qquad (2)$$

Since we will not address branching here, the set has to be reduced to 2D. This proceeds differently for the TDB classes and TDB-moments method, so we will perform this simplification and discuss the resulting equations twice.

TDB Classes Modeling

The 2-D version of the set population balances of Table 2 that is employed here follows by taking the sum over all branching numbers from $k = 0$ to ∞. Doing so is a simple operation yielding exactly the same set of equations, but with terms containing one index less. The absence of the aforementioned feedback of branching on kinetics is the direct cause for this simplicity. It is mathematically expressed by the absence of the branching index k as a factor in the original set of equations—in clear contrast to the TDB index i that appears in the living and dead chain contributions to the population balance from TDB propagation.

As a next step in the TDB classes model, the 2-D equations of Table 2 have to be transformed into a form employing separate 1-D distributions for dead and living chains with specific numbers of TDBs. To illustrate some aspects of this transformation, the 2-D version of the TDB propagation equations for living and dead chains is given (the $+=$ duet means a contribution to the overall balance equation of the respective species):

$$\frac{dR_{n,i}}{dt} += k_{db}(-R_{n,i}\sum_{n=1}^{\infty}\sum_{i=0}^{\infty} iP_{n,i} + \sum_{m=1}^{n-1}\sum_{j=0}^{i+1} jP_{m,j}R_{n-m,i-j+1}) \quad (3)$$

$$\frac{dP_{n,i}}{dt} += -k_{db} i\lambda_0 P_{n,i} \quad (4)$$

In the TDB classes model, we replace the 2-dimensional distributions $R_{n,i}$ and $P_{n,i}$ by a number I of distinct 1-dimensional distribution variables for living and dead chains: ${}^iR_n$ and ${}^iP_n$ ($i = 0..\ I - 1$). Equation 3 then is implemented in the Galerkin FEM code as a number of combination steps:

$${}^iR_n + {}^jP_m \xrightarrow{k_{db}j} {}^{i+j-1}R_{n+m} \quad (5)$$

If both i and j run from 0 to $I - 1$, this implies that eq 3 is equivalent to I^2 reaction equations between I living and I dead chain distributions. Similar large numbers are required for all of the bimolecular reactions between macromolecules: termination and transfer to polymer reactions. It is evident that this approach is limited to chains with few terminal double bonds. For the case of one TDB per chain at maximum, the system with $I = 2$, having population balances for ${}^0R_n$, ${}^1R_n$, ${}^0P_n$, and ${}^1P_n$, provides an exact solution. For the multiple TDB case, we will see that this model fails to describe longer chains, since these may carry numbers of TDB's much higher than $I - 1$. The advantage of the classes model is that it does not require an additional closure relationship, as we will be confronted with in the TDB moment approach. However, bimolecular reactions between macromolecules with a large number of TDB's have to be dealt with in an approximate way, e.g.:

$${}^{I-1}R_n + {}^{I-1}P_m \xrightarrow{k_{db}(I-1)} {}^{I-1}R_{n+m} \quad (5a)$$

In fact, this reaction should produce living chains belonging to the population of $2I - 1$ TDB's, but as the maximum is limited to $I - 1$, we thus assume them to be collected in the population of I TDB's. To conclude, the TDB classes model yields exact solutions, if we would be able to allow I to be unlimited. For practical reasons, however, we are forced to use a cutoff approach and limit I to values lower than 10. In our TDB classes model we have implemented the system with $I = 6$, yielding around 300 reaction equations, of which we will present results in the last section.

TDB Moments Model

Derivation of the Models. This approach follows the pseudo-distribution method developed for the bivariate MW/DB distribution of ldPE,[22] which basically reduces the 2-D problem to a 1-D problem by taking the moments of the branching distribution. In the present case, we start with the full 3-D set of Table 2 and then reduce it to a 1-D formulation by developing the TDB and branching moment expressions. The (N,M)th branching-TDB moment or pseudodistributions for living and dead chains are defined as

$$\Phi_n^{N,M} = \sum_{i=0}^{\infty} i^N (\sum_{k=0}^{\infty} k^M R_{n,i,k}) \quad \Psi_n^{N,M} = \sum_{i=0}^{\infty} i^N (\sum_{k=0}^{\infty} k^M P_{n,i,k}) \quad (6)$$

Performing the corresponding summations on the equations in Table 2, one obtains the (N,M)th moment formulation of Table 3. Some of the summation terms in these equations will not be evaluated for the general (N,M) case, but we will determine them by assigning values to N and M. Since in this article we will not address branching, we take $M = 0$ here, leaving the higher branching moment distribution for a forthcoming paper. We will focus now on the TDB moment distributions and successively derive the model equations for the zeroeth, first, and second moments, or $N = 0$, 1, and 2. Solving the model thus essentially means solving the populations balances of the real concentration distributions R_n and P_n and the pseudodistributions $\Phi_n^{N,M}$ and $\Psi_n^{N,M}$.

The resulting equations for $N = 0$ and $M = 0$ are listed in Table 4. Here, the (0,0)th moments are the usual 1-dimensional chain length distribution variables, defined as

$$R_n = \sum_{i=0}^{\infty}\sum_{k=0}^{\infty} R_{n,i,k} (= \Phi_n^{0,0}); \quad P_n = \sum_{i=0}^{\infty}\sum_{k=0}^{\infty} P_{n,i,k} (= \Psi_n^{0,0}) \quad (7)$$

All of the derivations are straightforward, but to the TDB propagation deserves closer examination. From Table 3, we have the general (N,M) formulation

$$\frac{d\Phi_n^{N,M}}{dt} += k_{db}\sum_{i=0}^{\infty} i^N \sum_{k=0}^{\infty} k^M (-R_{n,i,k}\sum_{n=1}^{\infty}\sum_{j=0}^{\infty}\sum_{l=0}^{\infty} iP_{n,j,l} + \sum_{m=1}^{n-1}\sum_{j=0}^{i+1}\sum_{l=0}^{k} jP_{m,j,l}R_{n-m,i-j+1,k-l-1}) \quad (8)$$

Taking $M = 0$ and $N = 0$, the first term in parentheses can be rewritten as

$$\sum_{i=0}^{\infty}\sum_{k=0}^{\infty}(R_{n,i,k}\sum_{n=1}^{\infty}\sum_{i=0}^{\infty}\sum_{k=0}^{\infty} iP_{n,i,k}) = \sum_{i=0}^{\infty}\sum_{k=0}^{\infty}(R_{n,i,k}\sum_{n=1}^{\infty}\Psi_n^{1,0}) = (\sum_{n=1}^{\infty}\Psi_n^{1,0})\sum_{i=0}^{\infty}\sum_{k=0}^{\infty} R_{n,i,k} = R_n\sum_{n=1}^{\infty}\Psi_n^{1,0} \quad (9)$$

The second term in parentheses can be rewritten as follows:

$$\sum_{i=0}^{\infty}\sum_{k=0}^{\infty}\sum_{m=1}^{n-1}\sum_{j=0}^{i+1}\sum_{l=0}^{k} jP_{m,j,l}R_{n-m,i-j+1,k-l-1} = \sum_{m=1}^{n-1}\{\sum_{k=0}^{\infty}\sum_{l=0}^{k}\sum_{j=0}^{\infty}(jP_{m,j,l}\sum_{i=j-1}^{\infty} R_{n-m,i-j+1,k-l-1})\} = \sum_{m=1}^{n-1}\Psi_m^{1,0}R_{n-m} \quad (10)$$

Thus, we find the TDB propagation term for the living chains to be

$$\frac{dR_n}{dt} += k_{db}(-R_{n,i,k}\sum_{n=1}^{\infty}\Psi_n^{1,0} + \sum_{m=1}^{n-1}\Psi_m^{1,0}R_{n-m}) \quad (11)$$

Applying $M = 0$ and $N = 0$ to the dead chains formulation yields

$$\frac{dP_n}{dt} += -k_{db}\lambda_0\Psi_n^{1,0} \quad (12)$$

Table 3. General (*N*,*M*)th Double Moment Formulation of the Population Balance Equation Set of Table 2, Obtained by Multiplying with the TDB Number and Branching Number Indices, i^N and k^M, and Subsequent Summation over These Indices

propagation	$\frac{d\Phi_n^{N,M}}{dt} = \frac{d\sum_{i=0}^{\infty} i^N \sum_{k=0}^{\infty} k^M R_{n,i,k}}{dt} += k_p M(\Phi_{n-1}^{N,M} - \Phi_n^{N,M})$
termination by disproportionation	$\frac{d\Phi_n^{N,M}}{dt} += -k_{td}\lambda_0 \Phi_n^{N,M}$
	$\frac{d\Psi_n^{N,M}}{dt} += \frac{1}{2}k_{td}\lambda_0(\sum_{i=0}^{\infty} i^N \sum_{k=0}^{\infty} k^M R_{n,i-1,k} + \Phi_n^{N,M})^a$
termination by recombination	$\frac{d\Phi_n^{N,M}}{dt} += -k_{tc}\lambda_0 \Phi_n^{N,M}$
	$\frac{d\Psi_n^{N,M}}{dt} += \frac{1}{2}k_{tc}\sum_{i=0}^{\infty} i^N \sum_{k=0}^{\infty} k^M (\sum_{m=1}^{n-1}\sum_{j=0}^{i}\sum_{l=0}^{k} R_{m,j,l} R_{n-m,i-j,k-l})$
transfer to monomer	$\frac{d\Phi_n^{N,M}}{dt} += -k_m M \Phi_n^{N,M};\quad \frac{d\Phi_1^{N,M}}{dt} += k_m \lambda_0 M$
	$\frac{d\Psi_n^{N,M}}{dt} += k_m M \Phi_n^{N,M}$
transfer to polymer	$\frac{d\Phi_n^{N,M}}{dt} += k_{tp}(\lambda_0 n \sum_{i=0}^{\infty} i^N \sum_{k=0}^{\infty} k^M P_{n,i,k-1} - \mu_1 \Phi_n^{N,M})$
	$\frac{d\Psi_n^{N,M}}{dt} += k_{tp}(-\lambda_0 n \sum_{i=0}^{\infty} i^N \sum_{k=0}^{\infty} k^M P_{n,i,k-1} + \mu_1 \Phi_n^{N,M})$
terminal double bond propagation	$\frac{d\Phi_n^{N,M}}{dt} += k_{db}\sum_{i=0}^{\infty} i^N \sum_{k=0}^{\infty} k^M (-R_{n,i,k}\sum_{n=1}^{\infty}\sum_{j=0}^{\infty}\sum_{l=0}^{\infty} i P_{n,j,l} + \sum_{m=1}^{n-1}\sum_{j=0}^{i+1}\sum_{l=0}^{k} j P_{m,j,l} R_{n-m,i-j+1,k-l-1})$
	$\frac{d\Psi_n^{N,M}}{dt} += -k_{db}\lambda_0 \Psi_n^{(N+1),M}$

[a] The first term in parentheses equals zero in the case where TDB creation by disproportionation is not accounted for.

Table 4. (0,0)th Moment Distribution Formulation of the Population Balance Equation Set of Table 3 (Taking $N = 0$ and $M = 0$)[a]

propagation	$\frac{dR_n}{dt} += k_p M(R_{n-1} - R_n)$
termination by disproportionation	$\frac{dR_n}{dt} += -k_{td}\lambda_0 R_n;\quad \frac{dP_n}{dt} += k_{td}\lambda_0 R_n$
termination by recombination	$\frac{dR_n}{dt} += -k_{tc}\lambda_0 R_n;\quad \frac{dP_n}{dt} += \frac{1}{2}k_{tc}\sum_{m=1}^{n-1} R_m R_{n-m}$
transfer to monomer	$\frac{dR_n}{dt} += -k_m M R_n;\quad \frac{dR_1}{dt} += k_m \lambda_0 M$
	$\frac{dP_n}{dt} += k_m M R_n$
transfer to polymer	$\frac{dR_n}{dt} += k_{tp}(\lambda_0 n P_n - \mu_1 R_n);\quad \frac{dP_n}{dt} += k_{tp}(-\lambda_0 n P_n + \mu_1 R_n)$
terminal double bond propagation	$\frac{dR_n}{dt} += k_{db}(-R_n \sum_{n=1}^{\infty} \Psi_n^{1,0} + \sum_{m=1}^{n-1} \Psi_m^{1,0} R_{n-m})$
	$\frac{dP_n}{dt} += -k_{db}\lambda_0 \Psi_n^{1,0}$

[a] This set is solved by the TDB moment distribution model.

The RHS expressions of eqs 11 and 12 contain higher TDB moment (1,0) distributions ($\Psi_n^{1,0}$) than the (0,0) moment distributions, R_n and P_n, they describe. This is a direct consequence of the fact that the reactivity of the dead chains depends on the number of TDB's they carry. Hence, at this point, we are already

Table 5. (1,0)th Moment Distribution Formulation of the Population Balance Equation Set of Table 3 (Taking $N = 1$ and $M = 0$)[a]

propagation	$\frac{d\Phi_n^{1,0}}{dt} += k_p M(\Phi_{n-1}^{1,0} - \Phi_n^{1,0})$
termination by disproportionation	$\frac{d\Phi_n^{1,0}}{dt} += -k_{td}\lambda_0\Phi_n^{1,0}$
	$\frac{d\Psi_n^{1,0}}{dt} += \frac{1}{2}k_{td}\lambda_0(\sum_{i=0}^{\infty} iR_{n,i-1} + \Phi_n^{1,0}) = k_{td}\lambda_0\left(\Phi_n^{1,0} + \frac{1}{2}R_n\right)$[b]
termination by recombination	$\frac{d\Phi_n^{1,0}}{dt} += -k_{tc}\lambda_0\Phi_n^{1,0}$; $\frac{d\Psi_n^{1,0}}{dt} += k_{tc}\sum_{m=1}^{n-1}\Phi_m^{1,0}R_{n-m}$
transfer to monomer	$\frac{d\Phi_n^{1,0}}{dt} += -k_m M\Phi_n^{1,0}$; $\frac{d\Phi_1^{1,0}}{dt} += k_m\lambda_0 M$
	$\frac{d\Psi_n^{1,0}}{dt} += k_m M\Phi_n^{1,0}$
transfer to polymer	$\frac{d\Phi_n^{1,0}}{dt} += k_{tp}(\lambda_0 n\Psi_n^{1,0} - \mu_1\Phi_n^{1,0})$
	$\frac{d\Psi_n^{1,0}}{dt} += k_{tp}(-\lambda_0 n\Psi_n^{1,0} + \mu_1\Phi_n^{1,0})$
terminal double bond propagation	$\frac{d\Phi_n^{1,0}}{dt} += k_{db}\{-\Phi_n^{1,0}\sum_{n=1}^{\infty}\Psi_n^{1,0} + \sum_{m=1}^{n-1}(\Psi_m^{2,0}R_{n-m} + \Psi_m^{1,0}\Phi_{n-m}^{1,0} - \Psi_m^{1,0}R_{n-m})\}$
	$\frac{d\Psi_n^{1,0}}{dt} += -k_{db}\lambda_0\Psi_n^{2,0}$

[a] This set is solved by the TDB moment distribution model. [b] The first term between brackets equals zero in the case where TDB creation by disproportionation is not accounted for.

confronted with the closure problem present in the TDB moment model, anticipating that solving these higher moments leads to even higher moments in the equations.

Next, we will derive the higher moment equations. For $N = 1$ and $M = 0$, we obtain the set of population balance equations for the pseudodistributions of order (1,0) as listed in Table 5. The termination by recombination equation is derived by developing the summation term as follows:

$$\frac{1}{2}\sum_{i=0}^{\infty} i(\sum_{m=1}^{n-1}\sum_{j=0}^{i} R_{m,j}R_{n-m,i-j}) = \frac{1}{2}\sum_{m=1}^{n-1}\sum_{j=0}^{\infty} R_{m,j}(\sum_{i=j}^{\infty} iR_{n-m,i-j}) = \frac{1}{2}\sum_{m=1}^{n-1}\sum_{j=0}^{\infty} R_{m,j}(\sum_{i=0}^{\infty}(i+j)R_{n-m,i}) = \frac{1}{2}\sum_{m=1}^{n-1}(\sum_{j=0}^{\infty} jR_{m,j}\sum_{i=0}^{\infty} R_{n-m,i} + \sum_{j=0}^{\infty} R_{m,j}\sum_{i=0}^{\infty} iR_{n-m,i}) = \frac{1}{2}\sum_{m=1}^{n-1}(\Phi_m^{1,0}R_{n-m} + R_m\Phi_{n-m}^{1,0}) = \sum_{m=1}^{n-1}\Phi_m^{1,0}R_{n-m} \quad (13)$$

This yields for the recombination contribution to the population balance

$$\frac{d\Psi_n^{1,0}}{dt} += k_{tc}\sum_{m=1}^{n-1}\Phi_m^{1,0}R_{n-m} \quad (14)$$

With respect to TDB propagation, by $M = 0$ and $N = 1$, the first term in parentheses becomes

$$\sum_{i=0}^{\infty}\sum_{k=0}^{\infty}(iR_{n,i,k}\sum_{n=1}^{\infty}\sum_{i=0}^{\infty}\sum_{k=0}^{\infty} iP_{n,i,k}) = \sum_{i=0}^{\infty}\sum_{k=0}^{\infty}(iR_{n,i,k}\sum_{n=1}^{\infty}\Psi_n^{1,0}) = (\sum_{n=1}^{\infty}\Psi_n^{1,0})\sum_{i=0}^{\infty}\sum_{k=0}^{\infty} iR_{n,i,k} = \Phi_n^{1,0}\sum_{n=1}^{\infty}\Psi_n^{1,0} \quad (15)$$

The second term, somewhat more complicated, becomes

$$\sum_{i=0}^{\infty} i\sum_{k=0}^{\infty}(\sum_{m=1}^{n-1}\sum_{j=0}^{i+1}\sum_{l=0}^{k} jP_{m,j,l}R_{n-m,i-j+1,k-l-1}) = \sum_{i=0}^{\infty} i\{\sum_{m=1}^{n-1}\sum_{j=0}^{i}(jP_{m,j}R_{n-m,i-j+1})\} = \{\sum_{m=1}^{n-1}\sum_{j=0}^{\infty}(jP_{m,j}\sum_{i=j+1}^{\infty} iR_{n-m,i-j+1})\} = \{\sum_{m=1}^{n-1}\sum_{j=0}^{\infty}(jP_{m,j}\sum_{i=0}^{\infty}(i+j-1)R_{n-m,i})\} = \sum_{m=1}^{n-1}(\sum_{j=0}^{\infty} j^2P_{m,j}\sum_{i=0}^{\infty} R_{n-m,i} + \sum_{j=0}^{\infty} jP_{m,j}\sum_{i=0}^{\infty}(i-1)R_{n-m,i}) = \sum_{m=1}^{n-1}(\Psi_m^{2,0}R_{n-m} + \Psi_m^{1,0}\Phi_{n-m}^{1,0} - \Psi_m^{1,0}R_{n-m}) \quad (16)$$

Thus, we find the TDB propagation term for the living and dead chains to be, respectively

$$\frac{d\Phi_n^{1,0}}{dt} += k_{db}\{-\Phi_n^{1,0}\sum_{n=1}^{\infty}\Psi_n^{1,0} + \sum_{m=1}^{n-1}(\Psi_m^{2,0}R_{n-m} + \Psi_m^{1,0}\Phi_{n-m}^{1,0} - \Psi_m^{1,0}R_{n-m})\} \quad (17)$$

$$\frac{d\Psi_n^{1,0}}{dt} += -k_{db}\lambda_0\Psi_n^{2,0} \quad (18)$$

Again, the earlier observed higher moments at RHS are observed.

We finally present the result for one higher moment distribution, $N = 2$, $M = 0$. First, the termination by recombination term is developed:

$$\frac{1}{2}\sum_{i=0}^{\infty} i^2\Big(\sum_{m=1}^{n-1}\sum_{j=0}^{i} R_{m,j}R_{n-m,i-j}\Big) = \frac{1}{2}\sum_{m=1}^{n-1}\sum_{j=0}^{\infty} R_{m,j}\Big(\sum_{i=j}^{\infty} i^2 R_{n-m,i-j}\Big) = \frac{1}{2}\sum_{m=1}^{n-1}\sum_{j=0}^{\infty} R_{m,j}\Big(\sum_{i=0}^{\infty}(i+j)^2 R_{n-m,i}\Big) = \frac{1}{2}\sum_{m=1}^{n-1}\Big(\sum_{j=0}^{\infty} j^2 R_{m,j}\sum_{i=0}^{\infty} R_{n-m,i} + \sum_{j=0}^{\infty} R_{m,j}\sum_{i=0}^{\infty} i^2 R_{n-m,i} + \sum_{j=0}^{\infty} jR_{m,j}\sum_{i=0}^{\infty} iR_{n-m,i}\Big) = \frac{1}{2}\sum_{m=1}^{n-1}(\Phi_m^{2,0}R_{n-m} + R_m\Phi_{n-m}^{2,0} + 2\Phi_m^{1,0}\Phi_{n-m}^{1,0}) = \sum_{m=1}^{n-1}(\Phi_m^{2,0}R_{n-m} + \Phi_m^{1,0}\Phi_{n-m}^{1,0}) \quad (19)$$

This yields for the recombination contribution to the population balance

$$\frac{d\Psi_n^{2,0}}{dt} += k_{tc}\sum_{m=1}^{n-1}(\Phi_m^{2,0}R_{n-m} + \Phi_m^{1,0}\Phi_{n-m}^{1,0}) \quad (20)$$

The first term in the equation describing TDB propagation is derived in a similar way as eq 14, while the second term follows from

$$\sum_{i=0}^{\infty} i\sum_{k=0}^{\infty}\left(\frac{dR_{n,i,k}}{dt}\right) = \sum_{i=0}^{\infty} i^2\sum_{k=0}^{\infty}\Big(\sum_{m=1}^{n-1}\sum_{j=0}^{i+1}\sum_{l=0}^{k} jP_{m,j,l}R_{n-m,i-j+1,k-l-1}\Big) = \sum_{i=0}^{\infty} i^2\Big\{\sum_{m=1}^{n-1}\sum_{j=0}^{i}(jP_{m,j}R_{n-m,i-j+1})\Big\} = \Big\{\sum_{m=1}^{n-1}\sum_{j=0}^{\infty}(jP_{m,j}\sum_{i=j+1}^{\infty} i^2 R_{n-m,i-j+1})\Big\} = \Big\{\sum_{m=1}^{n-1}\sum_{j=0}^{\infty}(jP_{m,j}\sum_{i=0}^{\infty}(i+j-1)^2 R_{n-m,i})\Big\} = \sum_{m=1}^{n-1}(\Psi_m^{3,0}R_{n-m} + \Psi_m^{1,0}\Phi_{n-m}^{2,0} + 2\Psi_m^{2,0}\Phi_{n-m}^{1,0} - 2\Psi_m^{2,0}R_{n-m} - 2\Psi_m^{1,0}\Phi_{n-m}^{1,0} + \Psi_m^{1,0}R_{n-m}) \quad (21)$$

The total contribution of TDB propagation to the population balance thus becomes

$$\frac{d\Phi_n^{2,0}}{dt} += k_{db}\{-\Phi_n^{2,0}\sum_{n=1}^{\infty}\Psi_n^{1,0} + \sum_{m=1}^{n-1}(\Psi_m^{3,0}R_{n-m} + \Psi_m^{1,0}\Phi_{n-m}^{2,0} + 2\Psi_m^{2,0}\Phi_{n-m}^{1,0} - 2\Psi_m^{2,0}R_{n-m} + - 2\Psi_m^{1,0}\Phi_{n-m}^{1,0} + \Psi_m^{1,0}R_{n-m})\} \quad (22)$$

For the dead chains we have

$$\frac{d\Psi_n^{2,0}}{dt} += -k_{db}\lambda_0\Psi_n^{3,0} \quad (23)$$

It is obvious that even higher TDB moment distribution balances can be constructed, but we will restrict ourselves to the ones developed for up until the second moments. When applying the TDB moment model, in principle two solution strategies are possible: one using the zeroeth and first TDB moments only and the second with zeroeth, first, and second TDB moments. In the first case we have to find a closure relationship for the second moment, in the second case, one for the third moment. In the following we show that the system becomes simpler in the case of a maximum one TDB per chain.

Closure Relations. We have adopted a simple form for these relationships:

$$\Psi_n^{2,0} = D_n\frac{\Psi_n^{1,0}}{P_n}\Psi_n^{1,0} \quad (24)$$

$$\Psi_n^{3,0} = D'_n\frac{\Psi_n^{2,0}}{\Psi_n^{1,0}}\Psi_n^{2,0} \quad (25)$$

Here the functions D_n and D'_n are in fact polydispersities of the branching moment distributions and in principle to be determined as functions of chain length n. Inserting these closure relations in eqs 17 and 18, with respect to eqs 22 and 23, reduces them to

$$\frac{d\Phi_n^{1,0}}{dt} += k_{db}\left\{-\Phi_n^{1,0}\sum_{n=1}^{\infty}\Psi_n^{1,0} + \sum_{m=1}^{n-1}\left[\Psi_m^{1,0}\Phi_{n-m}^{1,0} + \left(D_n\frac{\Psi_m^{1,0}}{P_n} - 1\right)\Psi_m^{1,0}R_{n-m}\right]\right\} \quad (17a)$$

$$\frac{d\Psi_n^{1,0}}{dt} += -k_{db}\lambda_0 D_n\frac{\Psi_m^{1,0}}{P_n}\Psi_n^{1,0} \quad (18a)$$

$$\frac{d\Phi_n^{2,0}}{dt} += k_{db}\left\{-\Phi_n^{2,0}\sum_{n=1}^{\infty}\Psi_n^{1,0} + \sum_{m=1}^{n-1}\left[\Psi_m^{1,0}\Phi_{n-m}^{2,0} + 2\Psi_m^{2,0}\Phi_{n-m}^{1,0} + \left(D'_n\frac{\Psi_m^{2,0}}{\Psi_m^{1,0}} - 1\right)\Psi_m^{2,0}R_{n-m} + - 2\Psi_m^{1,0}\Phi_{n-m}^{1,0} + \Psi_m^{1,0}R_{n-m}\right]\right\} \quad (22a)$$

$$\frac{d\Psi_n^{2,0}}{dt} += -k_{db}\lambda_0 D'_n\frac{\Psi_m^{2,0}}{\Psi_n^{1,0}}\Psi_n^{1,0} \quad (23a)$$

An exact determination of D_n and D'_n is not possible, but they can be estimated from results of the TDB classes model in regions with few TDBs per chain. We will discuss this along with other closure strategies in the Results section.

Maximum One Terminal Double Bond per Chain: Mathematical Equivalence of TDB Classes Model and TDB Pseudodistributions Model

Both the TDB classes and TDB moment model have been derived for the general case of an arbitrary number of TDBs per chain. Evidently, despite the differences in modeling approach, one hopes to arrive at identical results from the two models. However, due to the differences in dealing with the nonexact parts—closure

relations in the TDB moment distribution model and accounting for chains with more TDB's than accounted for in the TDB classes model—in general, results may deviate. However, one condition exists under which the two approaches lead to the same result: the case of a maximum one terminal double bond per chain.

Two mechanisms can be responsible for the occurrence of chains with more than one terminal double bond: insertion of chains with a TDB created by disproportionation termination and termination by recombination. In the case of PVAc, recombination is generally considered to be absent, while some discussion still exists about the reactivity of the 1,2-substituted TDB's created by disproportionation.[19] If this reactivity is negligible and recombination does not occur, chains may carry one TDB at a maximum. Until now, this is the only case being dealt with in modeling studies of PVAc.[1,6−13] Here, we will treat this case as well, but first see what happens to the TDB classes and TDB moments models as previously derived in the case of a maximum one TDB.

In the TDB classes model the set of population balance equations describes four distributions: ${}^0R_n$, ${}^1R_n$, ${}^0P_n$, ${}^1P_n$. This set can be solved in an exact way without additional assumptions. As for the TDB moments approach we notice that in the case of a maximum one TDB per chain all TDB moments higher than the zeroth moment become identical; from eq 6 we have, for $i \in \{0,1\}$

$$\Phi_n^{N,M} = \sum_{i=0}^{1} i^N \left(\sum_{k=0}^{\infty} k^M R_{n,i,k}\right) = \sum_{i=0}^{1}\sum_{k=0}^{\infty} k^M R_{n,i,k} = \Phi_n^{0,M} \quad (N = 0) \tag{26}$$

$$\Phi_n^{N,M} = \sum_{i=0}^{1} i^N \left(\sum_{k=0}^{\infty} k^M R_{n,i,k}\right) = \sum_{k=0}^{\infty} k^M R_{n,1,k} \quad (N > 0)$$

Thus, for $M = 0$ and $N = 0$ we find $R_n = R_{n,0} + R_{n,1}$, while for $M = 0$ and $N = 1$, it follows that $\Phi_n^{1,0} = \Phi_n^{2,0} = \Phi_n^{3,0} = ... = R_{n,1}$. In other words, the higher moments simply represent the concentration distribution of all the chains with a terminal double bond. Similarly, for dead chains we find that $P_n = P_{n,0} + P_{n,1}$ ($M = 0$, $N = 0$) and $\Psi_n^{1,0} = \Psi_n^{2,0} = \Psi_n^{3,0} = ... = P_{n,1}$.

This has important consequences for the model consisting of the population balances derived above. First, only the first TDB moment distributions, $\Phi_n^{1,0}$ and $\Psi_n^{1,0}$, have to be solved in addition to the real concentration distributions. Second, the TDB propagation contributions to the population balances become greatly simplified and their closure problem vanishes, since with $\Psi_n^{2,0} = \Psi_n^{1,0}$ eqs 17 and 18 become, respectively

$$\frac{d\Phi_n^{1,0}}{dt} + = k_{db}\left(-\Phi_n^{1,0}\sum_{n=1}^{\infty}\Psi_n^{1,0} + \sum_{m=1}^{n-1}\Psi_m^{1,0}\Phi_{n-m}^{1,0}\right) \tag{27}$$

$$\frac{d\Psi_n^{1,0}}{dt} + = -k_{db}\lambda_0\Psi_n^{1,0} \tag{28}$$

This implies that under the condition of a maximum one TDB per chain, the set of population balance equations of the TDB branching moment variant of the model is solvable without requiring any additional closure assumption. Moreover, one should notice that the distributions R_n and P_n of the moments model are identical to the sums of two distributions in the classes model ${}^0R_n + {}^1R_n$ and ${}^0P_n + {}^1P_n$, respectively. Similarly, the pseudodistributions $\Psi_n^{1,0}$ and $\Phi_n^{1,0}$ of the moments model are identical to ${}^1R_n$ and ${}^1P_n$, respectively, in the classes approach. Since solving the four distributions individually (classes model) or two of them individually and the other two included in a summation (moment model) should not make any difference, it follows that the two sets of population balance equations in fact are exactly equivalent.

Finally, we note that we derived a moment model based on the population balance equations of the TDB moment distribution model; this moment model is presented in the Appendix (see Supporting Information). We have done so to compare to previously constructed moment models for the PVAc case.[1,11,12] In such models the transfer to polymer reaction gives rise to a closure problem (see Appendix in Supporting Information), which we solved by general closure relationships provided by Hulburt and Katz.[25] Previous authors have dealt with this problem in different ways.

Kinetic Constants for the Base Case: Poly(vinyl acetate)

The base case used in the modeling work is the polymerization of *vinyl acetate*. Kinetic constants are assumed to be representative for polymerization of vinyl acetate in a CSTR at 60 °C, either in bulk or in solution (Table 8). The propagation constant k_p was taken from two literature sources.[20,26] Some uncertainty exists as to the termination rate. Most authors adopt disproportionation as the prevailing mechanism. In early work,[6,11−13] mostly dealing with solution polymerization, the system is considered to be transfer dominated, which means that chain length distributions do not depend on the termination rate coefficient, being completely determined by transfer reactions. Using our model, we found the distribution to become termination-independent for $k_{td} < 10^5$ m^3/(kmol·s). Consequently, we have adopted this value as the lower limit of the termination constant. More recently, much higher values are reported: k_{td} around 1.5×10^9 m^3/(kmol·s).[18] We consider this as the upper limit. A series of simulations has been carried out for the intermediate value of 10^8 m^3/(kmol·s). Data for the transfer reactions were taken from the same source,[18] which values appear to be commonly accepted in most PVAc modeling work. The base case value for the transfer to monomer rate coefficient k_m is assumed to be 2.34 m^3/(kmol·s). Regarding transfer to polymer the older references infer values for the ratio k_{tp}/k_p around 1.3×10^{-4}, based on observed branching frequencies of 0.0015 branch points per monomer unit inserted in polymer chains. Thus, in our case k_{tp} becomes 1.2 m^3/(kmol·s). However, from an NMR study,[19] much higher branching densities are found: around 0.01 branch points per monomer unit, corresponding to $k_{tp} = 10$ m^3/(kmol·s). Note that the relation between branching density and this rate constant is fairly straightforward.[19,22] Possible causes for the discrepancies are the differences in the branching measurement techniques, SEC/MALLS, rheometry or NMR, and in polymerization conditions. We will carry out simulations with $k_{tp} = 1.2$ and 10 m^3/(kmol·s) as the lower and upper limit and explore the sensitivity to this constant.

The terminal double bond propagation constant is usually estimated at 66% of the propagation rate constant[11] and we have adopted this value, $k_{db} = 6200$

Table 6. (1,0)th Moment Distribution Formulation of the Population Balance Equation Set of Table 3 (taking $N = 1$ and $M = 0$)

propagation	$\frac{d\Phi_n^{2,0}}{dt} += k_p M(\Phi_{n-1}^{2,0} - \Phi_n^{2,0})$
termination by disproportionation	$\frac{d\Phi_n^{2,0}}{dt} += -k_{td}\lambda_0\Phi_n^{2,0}$
	$\frac{d\Psi_n^{2,0}}{dt} += \frac{1}{2}k_{td}\lambda_0(\sum_{i=0}^{\infty} i^2 R_{n,i-1} + \Phi_n^{2,0}) = k_{td}\lambda_0\left(\Phi_n^{2,0} + \Phi_n^{1,0} + \frac{1}{2}R_n\right)^b$
termination by recombination	$\frac{d\Phi_n^{2,0}}{dt} += -k_{tc}\lambda_0\Phi_n^{2,0} \quad \frac{d\Psi_n^{2,0}}{dt} += k_{tc}\sum_{m=1}^{n-1}(\Phi_m^{2,0}R_{n-m} + \Phi_m^{1,0}\Phi_{n-m}^{1,0})$
transfer to monomer	$\frac{d\Phi_n^{2,0}}{dt} += -k_m M\Phi_n^{2,0}; \quad \frac{d\Phi_1^{2,0}}{dt} += k_m\lambda_0 M$
	$\frac{d\Psi_n^{2,0}}{dt} += k_m M\Phi_n^{2,0}$
transfer to polymer	$\frac{d\Phi_n^{2,0}}{dt} += k_{tp}(\lambda_0 n\Psi_n^{2,0} - \mu_1\Phi_n^{2,0})$
	$\frac{d\Psi_n^{2,0}}{dt} += k_{tp}(-\lambda_0 n\Psi_n^{2,0} + \mu_1\Phi_n^{2,0})$
terminal double bond propagation	$\frac{d\Phi_n^{2,0}}{dt} += k_{db}\{-\Phi_n^{2,0}\sum_{n=1}^{\infty}\Psi_n^{1,0} + \sum_{m=1}^{n-1}(\Psi_m^{3,0}R_{n-m} + \Psi_m^{1,0}\Phi_{n-m}^{2,0} + 2\Psi_m^{2,0}\Phi_{n-m}^{1,0} - 2\Psi_m^{2,0}R_{n-m} + - 2\Psi_m^{1,0}\Phi_{n-m}^{1,0} + \Psi_m^{1,0}R_{n-m})\}$
	$\frac{d\Psi_n^{2,0}}{dt} += -k_{db}\lambda_0\Psi_n^{3,0}$

[a] This set is solved by the highest TDB moment version of the TDB moment distribution model. [b] The first term between brackets equals zero in the case where TDB creation by disproportionation is not accounted for.

Table 7. (1,0)th Moment Distribution Formulation of Part of the Population Balance Equation Set of Table 5

termination by disproportionation	$\frac{d\Psi_n^{1,0}}{dt} += k_{td}\lambda_0\Phi_n^{1,0}$
terminal double bond propagation	$\frac{d\Phi_n^{1,0}}{dt} += k_{db}(-\Phi_n^{1,0}\sum_{n=1}^{\infty}\Psi_n^{1,0} + \sum_{m=1}^{n-1}\Psi_m^{1,0}\Phi_{n-m}^{1,0})$
	$\frac{d\Psi_n^{1,0}}{dt} += -k_{db}\lambda_0\Psi_n^{1,0}$

[a] These are valid for the case of one TDB per chain at maximum and obtained from the corresponding equations in table 5 by putting: $\Psi_n^{2,0} = \Psi_n^{1,0}$. This set is solved by the TDB moment distribution model for the one-TDB case, together with the other (unchanged) equations of Table 5.

Table 8. Rate Constants and Reactor Conditions for the Base Case

rate constant	value
k_d [1/s]	$9\ 10^{-6}$
k_p [m^3/(kmol·s)]	9500
k_{tc} [m^3/(kmol·s)]	0
k_{td} [m^3/(kmol·s)]	10^5 to 1.5×10^9
k_S [m^3/(kmol·s)]	0.34
k_m [m^3/(kmol·s)]	2.34
k_{db} [m^3/(kmol·s)]	500−6200
k_{tp} [m^3/(kmol·s)]	1.2−10
residence time τ (s)	4000
monomer (kmol m^{-3})	9 (bulk), 3 (solution)
initiator feed (kmol m^{-3})	depending on conversion and termination rate constant
chain transfer agent (kmol m^{-3})	6

m^3/(kmol·s), for our base case as well, but again vary it in our simulations. It should be noted that some confusion exists in the literature regarding the interpretation of the constant k_{db}. The reaction equation eq 1 immediately makes clear that the reaction rate is proportional to the number of TDBs on the dead chain involved, meaning, for instance, that it equals zero for dead chains without TDB. Some earlier studies[1,6−10] do account for this proportionality, but others do not by using the simplified reaction equation[11]

$$R_n + P_m \xrightarrow{k_{bd}^*} R_{n+m} \tag{29}$$

Assuming $k_{db}^* = k_{db}$ would overestimate the reactivity for dead chains with zero TDB and underestimate it for chains with more than one. Although under certain circumstances, depending on the TDB distribution, this assumption might be valid, but in general, it is not. The correct value of k_{db} would in principle directly follow from a measured TDB distribution. In the case of a maximum one TDB per chain, this is the fraction dead chains carrying a TDB, since for this fraction, x_{TDB}, Tobita[11] derived (x is monomer conversion, $\bar{n}_n$ number-average chain length)

$$x_{TDB} = \frac{k_m/k_p}{1 + k_{db}/k_p\left(\frac{x}{1-x}\right)}\bar{n}_n \qquad (30)$$

However, no such experimental data on x_{TDB} are available, so the value of k_{db} has to be determined in an indirect way, e.g., from a measured MWD. For the time being, we have adopted the value of k_{db} for the base case that is mostly used.[6−11]

Results: Maximum One TDB per Chain

Comparison to Previous Work on Molecular Weight Distribution Modeling. All the results in this section have been obtained using the TDB moment model that has been derived for the case of a maximum one TDB per chain, since this is the (implicit) assumption in earlier studies. The set of equations used is presented in Table 5, except for those describing disproportionation and TDB propagation, which for the 1-TDB case become more simplified; the latter are listed in Table 7. We start with a comparison to earlier experimental[11] and modeling (Monte Carlo[9]) work. Both studies address the case of vinyl acetate polymerization in *tert*-butyl alcohol in a solvent−monomer ratio of 2:1. Under these circumstances, termination is considered to be dominated by transfer reactions. This means that although radical concentration and conversion still are determined by the disproportionation termination, the chain length distribution becomes independent of this termination mechanism. In our simulations, we found this to be the case for values of termination constants k_{td} up to 10^5 m^3/(kmol·s). To stay as close as possible to the simulation conditions of the mentioned modeling reference,[9] we adopted this k_{td} value to perform this series of simulations with.

The results for the number and weight-average chain length as varying with conversion are shown in the plots of Figure 4. From this figure, it becomes evident that using the same kinetic data set as the refs 9 and 11 gives good agreement at low conversion but increasing deviation at higher conversion. The calculated MWD (no experimental MWD are yet available) is compared to the model results by Tobita, and we observe good agreement at low conversion (Figure 5). At high conversion, our MWD features a long tail at high chain length that is not predicted in the Monte Carlo study.[9] This difference is wholly due to the difference in modeling approach, since all kinetic constants are the same and also the interpretation of k_{db} is identical. It should be noted that our result is based on an exact solution of the population balances without any additional assumption. The difference in weight-average chain length between a moment model[11] and the Monte Carlo model[9] is attributed by the author of the latter work to the existence of polyradicals, not being accounted for in the moment model. In our modeling approach we do not account for polyradicals either. We cannot definitively exclude this as a possible cause for the long tail in the dead chain distribution. However, in view of the very low concentration of the macroradicals as compared to the dead chain concentration, even at the longest chain lengths, we do not expect this to be the real cause. In a future publication dedicated to polyradicals, we will revisit this problem. Another explanation for the discrepancy between experimental and model results may be found in the uncertainty regarding the value of the TDB propagation rate constant k_{db}. Since no data are

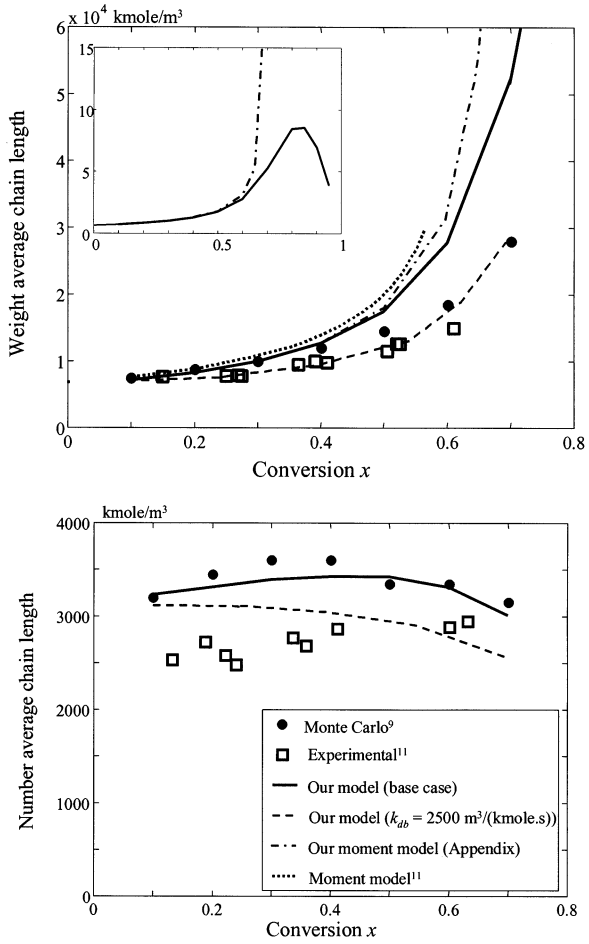

Figure 4. Comparison of number- and weight-average chain lengths predicted by our model as compared to experimental[11] and Monte Carlo simulations.[9] The inset in the $\bar{n}_w$ graph shows the limiting behavior of our model's $\bar{n}_w$ prediction at high conversion. For Appendix, see Supporting Information.

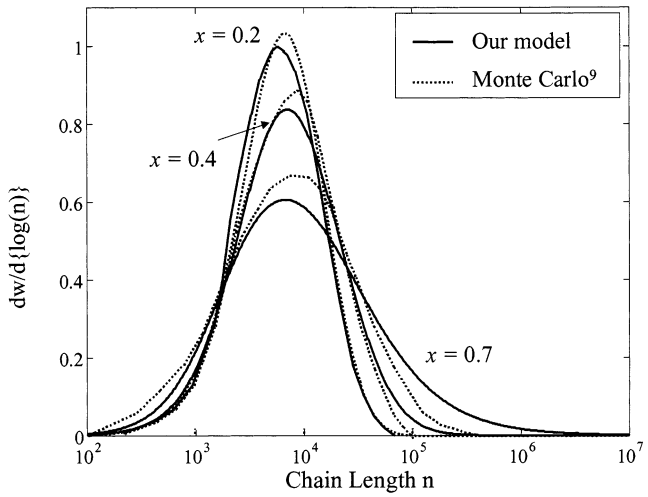

Figure 5. Comparison of chain length distributions predicted by our model as compared to Monte Carlo simulations.[9]

available on the fraction of dead chains with a TDB, x_{TDB}, we treated this rate constant as a parameter to be identified by fitting the model to the experimental data. Doing so we find $k_{db} = 2500$ m^3/(kmol·s) to produce fair agreement, as is seen from Figure 4. This implies that the value for k_{db} that has been used by most authors before, 6200 m^3/(kmol·s), turns out to be too high to provide good agreement between our model and

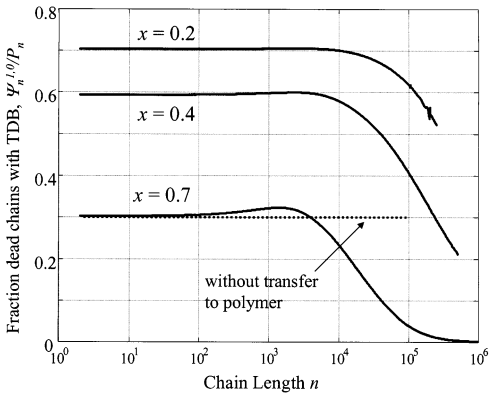

Figure 6. Fraction of dead chains with a terminal double bond, $\psi_n^{0,1}/P_n$, vs chain length for various conversion levels. Average fractions, $\sum \Psi_n^{1,0}/\sum P_n$: $x = 0.2$, 0.705; $x = 0.4$, 0.594; $x = 0.7$, 0.303. These are in agreement with eq 29. Without the transfer to polymer reaction, no decline is observed.

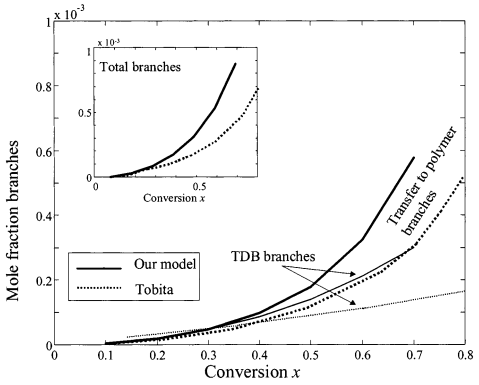

Figure 7. Mole fraction of branch points on monomer units inserted vs monomer conversion. Branches created by terminal double bond propagation and by transfer to polymer are plotted separately. The inset shows the total branching vs conversion.

experimental molecular weight data. Previous modeling efforts for the CSTR case gave rise to similar conclusions,[9] although for the batch case, good agreement has been found when assuming $k_{db} = 6200$ m^3/(kmol·s).[11]

The results of moment modeling have also been presented in Figure 4. Our and previous moment models[11,12] feature good agreement with the full Galerkin FEM approach until conversions of 50%, but strongly deviate at higher conversion. The older moment models predict somewhat higher values for the weight-average chain length. The upper limit of convergence (second moment $\rightarrow \infty$), which has been interpreted as a "gelpoint", is situated at 68% for the older moment model,[12] where our moment model has 79% as the upper limit. This confirms our earlier findings[2] that assumptions in moment models (closure relations) strongly influence the outcomes. Quite remarkably, when exploring the very high conversion region, the full Galerkin FEM model features a maximum in the $\bar{n}_w$ at around 85% conversion, as can be seen in the inset of Figure 4. The Monte Carlo simulations did not predict such a maximum, but then these were not extended to these high conversion values.

Comparison to Previous Work on TDB Distribution and Branching Modeling. The results concerning the fraction of chains with a terminal double bond are shown in the TDB fraction vs chain length plot of Figure 6. Comparison to earlier work is only possible for the average fraction chains with a TDB, which in the Monte Carlo model[9] follows eq 29. In this respect, we find perfect agreement. Hence, the Monte Carlo and our Galerkin FEM approaches are essentially equal as far as TDB insertion frequency is concerned. Consequently, in view of the observed differences in chain length distribution, these now can be more precisely attributed to the way the impact of TDB insertion frequency on chain length distribution is accounted for. According to our results and eq 29, the fraction TDB decreases with conversion. This phenomenon can be attributed to fact that higher conversion implies higher macroradical concentrations. If the available chains with a TDB are distributed among a higher number of growing chains, at higher conversion, their insertion frequency per chain obviously decreases. We also observe a lower TDB content of the longer chains. This is logical in view of the following argument. The flat profile of the curve is typical for the propagation dominated lower part of the chain length range. Here, living chains without TDBs, created by initiation and transfer to solvent, and with TDBs, created by transfer to monomer, grow by propagation in exactly the same manner. The longer chain length range, in contrast, is dominated by transfer to polymer, meaning that the major part of living chains produced is created by this reaction, rather than by propagation. Now, both the dead chains without and with TDB are attacked by this transfer reaction, but in the case of the TDB carrying dead chains this occurs in competition with the TDB propagation. As a consequence of the competition, relatively less living chains with a TDB are formed. Through the repeated action of termination and reactivation this effect is amplified and results in a decline of the number of TDBs on both living and dead chains. To the support of this explanation we carried out a simulation with zero transfer to polymer. As seen in Figure 6, under these conditions indeed the flat profile is extended to a region of vanishing concentration and no decline is observed. Note that the chain length distribution now is much narrower (polydispersity 2.9).

In this case of poly(vinyl acetate), branches are the result from both transfer to polymer and TDB propagation. It is interesting to see which fraction is created by either mechanism, as has been done before.[9] The result is shown in Figure 7, which also offers the possibility to compare it with previous work. We observe branching to increase with conversion, where the increase of the transfer to polymer related branches is most pronounced, according to both studies. This implies that the ratio between the TDB and the transfer branches increases with conversion from roughly 1:1 to 1:2. The only deviation found between the studies is the higher absolute level of branching (50% higher) found by us. This is consistent with the stronger tailing of the molecular weight distributions predicted by our model in comparison with the previous work. Again, no other explanation can be given for this discrepancy than the difference in the modeling approach, since the assumed kinetics is identical in both studies.

Sensitivity Study: Asymptotic Behavior, Bimodal CLD, Gel Formation, and High Macroradical Concentrations

Sensitivity to Disproportionation and Transfer to Polymer. The objective of this part is to explore the sensitivity of our model to changes in assumptions about kinetic mechanisms and parameters and other conditions. In Figures 8 and 9, we show the chain length

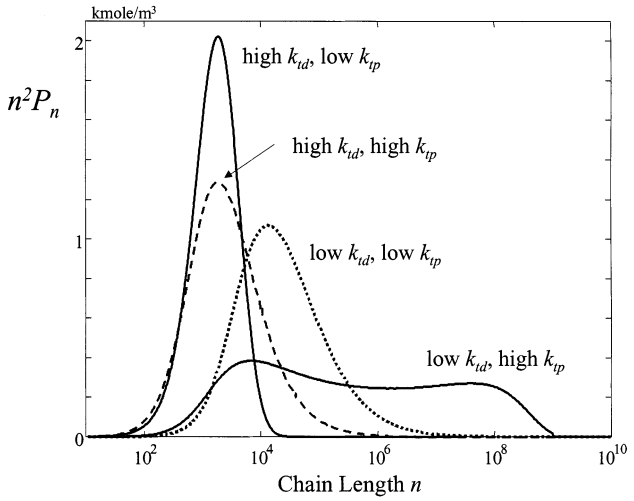

Figure 8. Sensitivity of molecular weight distribution to disproportionation termination and transfer to polymer: $k_{td} = 10^5$ m³/(kmol·s) (low), 1.5×10^9 m³/(kmol·s) (high); $k_{tp} = 1$ m³/(kmol·s) (low), 10 m³/(kmol·s) (high). Conversion in all cases was 50%.

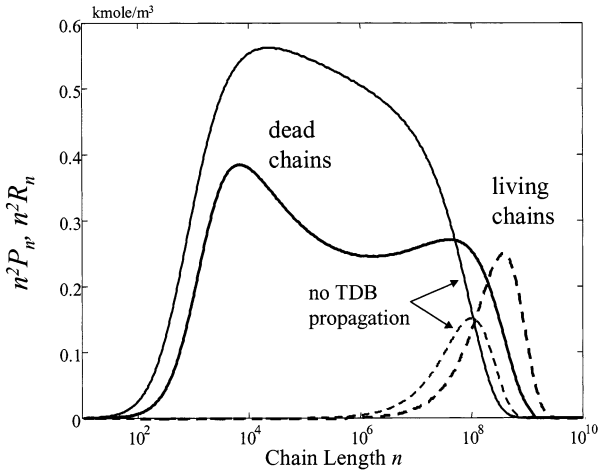

Figure 9. Chain length distributions of dead and living chains for the case of low k_{td} (10^5 m³/(kmol·s))/high k_{tp} (10 m³/(kmol·s)) with and without TDB propagation. At long chain lengths living chain concentration exceeds dead chain concentration. Conversion in both cases was 50%.

distributions for combinations of high and low values of the disproportionation ($k_{td} = 1.5 \times 10^9$ and 10^5 m³/(kmol·s), respectively) and transfer to polymer constants ($k_{tp} = 1$ and 10 m³/(kmol·s), respectively). A lower disproportionation constant not only leads to longer average chain lengths, but also to broader distributions. Stronger transfer to polymer also leads to broadening. These results, and in particular the very broad distribution obtained for the lower limit of k_{td} and the upper limit of k_{tp}, are of interest from several points of view that we will discuss subsequently, partially to the background of earlier work:

- Some distributions extend unto very long chain lengths, which is relevant for gelation.
- Some distributions possess a pronounced bimodality.
- The bimodal distributions of dead chains correspond to extremely high concentrations of living chains at long chain lengths, even exceeding dead chain concentration (Figure 9), which is relevant for our discussion concerning multiradicals.

These interesting phenomena exist for a particular combination of kinetic constants that have not yet been verified with hard experimental data. However, it is still interesting to explore this situation, since it yields information on the asymptotic behavior to which certain mechanisms give rise when becoming very strong. This might be of practical importance for other systems. We will examine the results in a systematic way by checking whether the observed phenomena only occur in the kinetically complex situation of transfer to polymer and TDB propagation. Therefore, we also performed simulations for the simpler case of radical polymerization in a CSTR with transfer to polymer and recombination termination in absence of TDB propagation reactions (see, e.g., Figure 9).

Long Chain Lengths: The Gelation Regime. The asymptotic behavior is characterized by very broad distributions extending into an extremely long chain region. In this respect, our findings are also important in the context of gel formation, a topic addressed by us in an earlier study.[2] It should be noticed that now we are able to arrive at reliable solutions of the problem despite the highly extended chain length domain. In the earlier work on chain length modeling under gelling conditions, such extended domains seemed to be unattainable for computational reasons, which was a reason for introducing a "cutoff limit". Because of a more efficient treatment of bimolecular reactions, which employs a subsummation of products of very broad distributions,[24] at present we are able to successfully deal with long-tail problems without using the cutoff approach. The results of the cutoff approach are still valid, but under the present state-of-the-art, its applicability has shifted to considerably longer chain lengths. As to the treatment of chain length modeling in the gel regime, this implies that we still might be confronted with chain length regions unattainable for exact modeling. This then still would force us to use a cutoff approach, which will indeed turn out to be so in the case of more than one TDB per chain. However, in the case of one TDB per chain our model yields solutions without requiring closure relations covering chain lengths up until 10^{10}. Now, these are well within a region that usually is considered as a gel regime. This interestingly implies that our model, under these kinetic circumstances, is able to fully characterize a gel polymer in terms of chain length and TDB distribution (later also branching distributions). The question then obviously rises, which part of the polymer is the gel polymer, but this is a matter of completely different nature, since this is depends from the definition of what a gel is. In size exclusion chromatography, a gel fraction is the fraction of polymer that is insoluble, which depends on solvent and temperature. The solubility characteristics are a matter of solid−liquid equilibrium and have to be studied by thermodynamics, which is beyond the scope of this article. However, in principle, if one knows these characteristics and measures the gel weight fraction, then comparing the chain length distribution as measured with SEC to the modeled one provides us with sufficient information to characterize such a gel fraction.

Finally, we analyze our results to earlier views and conclusions regarding the probability of gel formation. Monte Carlo simulations of poly(vinyl acetate)[9] did not produce evidence for gel formation, since the CLDs found were not very broad (Figure 5). However, in another study,[27] it was put forward that in principle systems with a combination reaction like TDB propagation may give rise to gel formation, whereas those

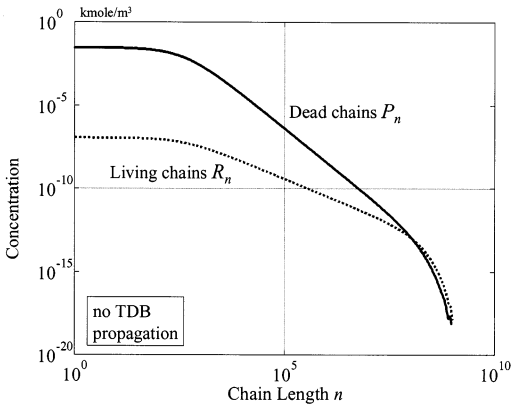

Figure 10. Double logarithmic plot of dead and living chain concentration vs chain length for the case of low k_{td} and high k_{tp} in absence of TDB insertion. The change from a linear to a curved shape at high chain length is attributed to the change in contributions of propagation and transfer to polymer, according to eq 3. Conversion was 50%.

without combination would not at all. This is partially in line with our results (Figure 9), since we find broadening due to TDB propagation, although we then merely conclude that a gradual difference exists between the two systems rather than a fundamental one. Moment modeling for a system with transfer to polymer and TDB propagation has been performed, which gave rise to conclusions about gel formation.[1] A comparison here is not fully possible, since the mentioned study has dealt with batch reactors only. An extensive comparison between moment and Galerkin FEM modeling including batch reactors has been given in our earlier work.[2]

Bimodal CLD and High Macroradical Concentration. Here, again, we compare the CLD of the case with TDB propagation to that obtained in absence of this mechanism (Figure 9). These situations apparently have the two striking features of a bimodal CLD *and* higher living chain than dead chain concentrations at long chain lengths in common. It will turn out that these two phenomena are interrelated, so we discuss them here together. In our cutoff modeling study, we already discussed the issue of living chain concentrations being higher than that of dead chains, but here we show its numerical proof. In addition, this finding responds to various issues raised in gelation context before. The first is the idea that the longest chains (gel chains) are more likely living chains,[28] which is now confirmed by our model. Second is the issue of multiradicals, which will not be dealt with in a conclusive way in this paper, but still we will give some remarks here. Anticipating our future publication on the topic of multiradicals, we notice the importance of the concentration ratio between living and dead chains. As long as this is much lower than unity, we should not bother about multiradicals. However, as they become of the same order of magnitude, multiradicals may play an important role. Consequently, this implies that in situations as depicted in Figure 9 (long chain lengths; concentrations of living higher than dead chains), the presence of multiradicals might alter the picture considerably. However, here we will restrict ourselves to monoradicals only and revisit the multiradicals later.

To examine the living and dead chain concentration as functions of chain length more quantitatively, we plot the dead and living chain concentration in a double-logarithmic plot, Figure 10. We observe straight lines at intermediate chain lengths, but a clear transition to steeper descent right at the chain length where the living and dead chain concentrations become of the same order of magnitude. We state that this decline is not a coincidence but has to be present necessarily. To understand this, one should note that the slope of the living chains in the linear part before the decline is such that continuation for $n \rightarrow \infty$ would cause the summation $\sum_{n=1}^{\infty} nR_n$ (λ_1) also to go to infinity, which would imply that a converged solution is not achievable. In that case, the curve in the semilogarithmic n^2R_n vs n plot would always continue to increase instead of showing a maximum and a decline to zero. Since the population balances are correctly solved until L, λ_1 must be finite; hence, the slope of R_n *must* feature a decline beyond L.

In addition, we should realize that the bimodality observed in the semilogarithmic plot has to be attributed to the discussed change in the curvature of the concentration distributions at high chain lengths. Notice that bimodal CLDs have been discussed before in this context[23] but then with a random scission mechanism playing a role. Yet two marked differences exist with respect to this situation. First, it occurs at much shorter chain lengths, and second, this happens in a situation where the macroradical concentration is still considerably lower than that of the dead chains.

Effect on CLD and TDB Distribution of TDB Propagation Rate and Conversion. The effect of TDB propagation rate constant and conversion on the distributions of chain length and fraction chains with a TDB has been assessed for intermediate values of the disproportionation and transfer to polymer rate coefficients: $k_{td} = 10^8$ m^3/(kmol·s); $k_{tp} = 5$ m^3/(kmol·s). In view of the ranges reported earlier, these values may be considered as being fairly realistic for PVAc. From the calculations (not shown, see Supporting Information), we conclude that the trends observed earlier under the limiting values of the mentioned kinetic constants persist here. Stronger TDB propagation leads to broadening of the CLD and lower values of the fraction chains with TDB. The latter phenomenon is easily explained by the fact that a higher k_{db} implies a higher reactivity of TDBs, and consequently they are more likely to be inserted. CLD is again seen to broaden with increasing conversion, while the fraction of dead chains with TDB decreases. The latter phenomenon is due to higher macroradical concentration and less frequent insertion of TDBs.

Results: More Than One TDB per Chain

In this section, results are discussed for the case of *active* TDB generation by disproportionation termination. This implies that none of the terms in Tables 2−6 associated with disproportionation are zero this time. In addition, Table 7 with the simplified balance equations, is not valid. We will first compare results from the TDB classes and the TDB moment model, since these are different for this case of an arbitrary number of TDBs per chain. Subsequently, the outcomes of the TDB moment models either including or not including the second TDB moment distribution will be discussed. Finally, the results will be shown of simulations with different rate constants for TDB propagation and termination by recombination or disproportionation. The latter will be compared to the findings of the maximum one TDB case of the previous secton.

Comparison of TDB Classes and TDB Moment Model. A comparison of the results will be made from

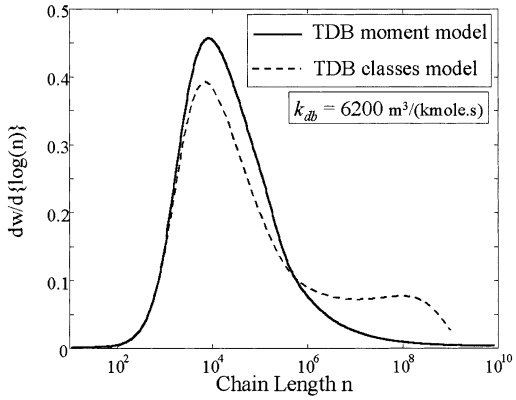

Figure 11. Comparison of chain length distribution from TDB classes and TDB moment model for standard conditions and $k_{db} = 6200$ m³/(kmol·s).

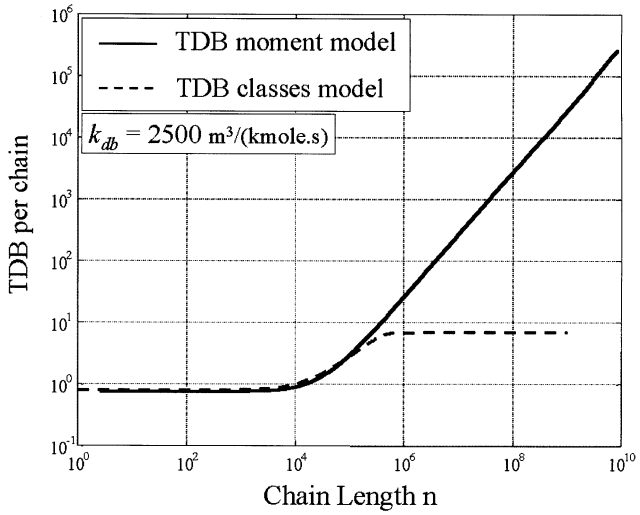

Figure 12. Comparison of average terminal double bond per chain as a function of chain length from TDB classes and TDB moment model for standard conditions.

the TDB classes model and the TDB moment model. For the latter the version with a closure relation for the third TDB moment distribution has been chosen, where we simply take:

$$D'_n = 1 \quad \text{for all } n \tag{31}$$

The results for the dead chain CLD are shown in Figure 11 for $k_{db} = 6200$ m³/(kmol·s), which reveals a significant difference. Differences for lower k_{db} are less important. The discrepancy between the two outcomes can be explained by regarding the average number of TDBs per chain as a function of chain length for the dead chains as depicted in Figure 12. Again we compare the outcomes from the two models, and it becomes immediately clear that the TDB classes model largely underestimates the number of TDBs per chains from chain lengths of 10^5 and higher. By restricting the classes model to describe distributions with up to seven TDBs per chain, we obviously find a maximum of seven TDBs per chain, which is at a chain length of around 10^5, according to both models. Beyond that, the TDB moment model predicts a linear increase of TDBs per chain with chain length in the double-logarithmic plot. The curves for other values of k_{db} practically coincide with the one shown for $k_{db} = 2500$ m³/(kmol·s). What we conclude from this is that according to the moment model dead

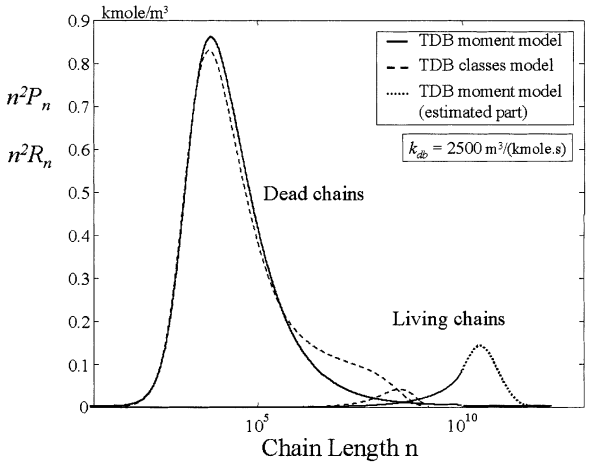

Figure 13. Comparison of chain length distributions for dead and living chains from TDB classes and TDB moment model for standard conditions. The part of the living chain CLD from the TDB moment model beyond 10^{10} is estimated (dotted curve) from the fraction monomers contained in living chains of 0.07 (see Figure 4).

chains with lengths departing from 10^5 contain a lot more TDBs and hence are much more reactive than the classes model predicts it. Being more reactive in the moment model implies that the longer dead chains are consumed to a greater extent than they are according to the classes model. This means that the concentration of long dead chains is much lower in the moment model than in the classes model, which is exactly what we observe in Figure 11. Another interesting aspect associated with the high reactivity of the long dead chains carrying many TDBs is the living chain concentrations and CLDs to which this gives rise. In Figure 13, the CLDs of the living chains from the two models are shown next to those of the dead chains. The one predicted by the moment model is shifted toward much longer chain lengths. Evidently, the high reactivity of the long dead chains also leads to an intensified TDB propagation process leading to a stronger growth of the living chains as well. It is even located at chain lengths longer than 10,[10] which we had to adopt here as a cutoff limit, so that the living CLD shown in Figure 13 is in part an extrapolated one (dotted curve). A discussion of using cutoff limits follows in the next section. Not only the length, but also the concentration of the living chains in the CSTR is higher according to the TDB moment model. In many cases, this fraction is negligible, but here it is not. According to the moment model with increasing TDB propagation rate, this fraction can amount to 18%. Such an increase is predicted by the classes model as well, but to a lesser extent. From this part, we conclude that the classes model greatly falls short in correctly describing the high numbers of TDBs per chain and the higher reactivity of dead chains as a consequence of this. Obviously, we therefore prefer the TDB moment model for the case of more than one TDB per chain. This is in sharp contrast to the situation of one TDB per chain at maximum, where we found the classes model and the moment distribution model to be equivalent.

We should now discuss the closure assumption made in the TDB moment model by assuming $D_n = 1$, eq 31. In fact, D_n and D'_n as defined in eqs 24 and 25 are polydispersities and can be calculated as functions of n from the TDB classes model. This is realized by extract-

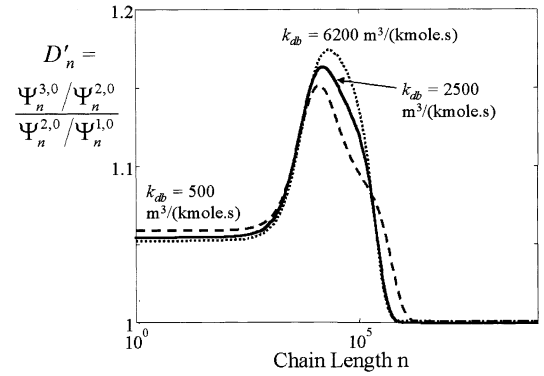

Figure 14. Polydispersity D'_n as a function of chain length for various k_{db} from the TDB classes model.

ing the leading TDB moments from the separate distributions as follows:

$$P_n = \sum_{i=0}^{I} {}^iP_n; \quad \Psi_n^{1,0} = \sum_{i=0}^{I} i({}^iP_n); \quad \Psi_n^{2,0} = \sum_{i=0}^{I} i^2({}^iP_n); \quad \Psi_n^{3,0} = \sum_{i=0}^{I} i^3({}^iP_n) \quad (32)$$

The result is given in Figure 14 for D'_n (for D_n; see Supporting Information). It should be realized that this figure gives a realistic picture over a limited chain length range only, e.g., until 10^5, in view of the maximum number of classes employed. We observe that the calculated D'_n is a weak function of n indeed, but it does not deviate strongly from one. It shows a maximum at chain length 10^4 and a subsequent fall to one, albeit on the edge of the validity range. Since in the TDB moment model the second TDB moment distribution $\Psi_n^{2,0}$ is explicitly used as a variable, it is possible to compute the polydispersity D_n and compare it to the one calculated from the classes model. For the highest k_{db} the maximum turns out to be unrealistically high. We attribute this to the $D_n = 1$ assumption, which most strongly deviates from the true D_n (Figure 14) at precisely the same chain length. Realizing that the more important TDB moment is $\Psi_n^{1,0}$, since it determines the reactivity for TDB propagation of the dead chains, we do not expect that a more precise prediction of the second moment will considerably change the outcomes as regards the first one. Consequently, we conclude that the assumption $D'_n = 1$ is acceptable for our purposes here.

The TDB moment distribution modeling approach can be employed in a lower and a higher TDB moment mode. The lower moment mode means solving the population balances of Tables 4 and 5 and applying a closure relationship for the second TDB moment distribution $\Psi_n^{2,0}$, while in the higher moment mode, balance equations of Tables 4−6 are solved, requiring a closure for the third TDB moment $\Psi_n^{3,0}$. We compared the results of the two approaches for both CLD and TDB distribution (see Supporting Information). It turns out that the higher closure model performs slightly better, so it is this model that we will use for simulations.

Using Cutoff Modeling in the Higher TDB Moment Model. Here, we discuss the results of the higher TDB moment model regarding chain length and TDB distributions. Figure 15 shows CLDs of both living and dead chains. Living CLDs for k_{db} higher than 500 m³/(kmol·s) fall beyond the cutoff limit, $L = 10^{10}$, that we had to use here. In earlier work,[2] we introduced the concept of a cutoff limit in CLD modeling. Because of the earlier mentioned improvement in the handling of product summations, we were able to shift the cutoff limit from 10^6 to 10^{10}. Now, it is important to note that at this extremely long chain length the model predicts the living chain concentration to be much higher than the dead chain concentration. This has strong implications for the discussion that we have raised in our aforementioned article about the question, which fraction of the monomer units is present in living chains longer than the cutoff limit L and which fraction exists in similar dead chains. This fraction turns out to be largely belonging to the living chains beyond L. It can be calculated in a simple manner. We start by taking the difference between the amount of monomer units converted ($M_{in} - M$) and the first moment of the dead chains, μ_1, representing the number of units in dead chains, which yields the total amount of units in living chains, λ_1. Now, taking the amount of monomer units present in the modeled part of the living CLD until $L = 10^{10}$, λ_1', and subtracting this from λ_1 yield the portion λ_1^h beyond the cutoff limit. Another issue raised in cutoff CLD modeling is concerned with the summation terms of concentration distributions over the full chain length range, or over parts of it beyond L.[2] This could be dealt with using corrections of certain moments. Regarding the population balance equation set presented in Tables 4−6 and following the line of thought of our previous work,[2] one sees that we should ensure to work with the complete moments λ_0, μ_1, and $\sum_{n=1}^{\infty} \Psi_n^{1,0}$. As for λ_0, our calculations show that no correction is needed, even when λ_1^h is significant with respect to λ_1. Furthermore, from the previous discussion on the presence of monomer units in living or dead chains longer than L, it is clear that no correction for μ_1 is required either. Finally, calculations show that a negligible part of the $\Psi_n^{1,0}$ distribution falls beyond L. In conclusion, all the full moments required are properly accounted for and no corrections are needed. Hence, all the population balances are correctly solved until the cutoff limit $L = 10^{10}$.

In our previous work,[2] we employed Flory distributions to estimate parts of the distributions falling beyond L. Here, we adopt a different, double-logarithmic, extrapolation procedure, not to estimate correction terms, which is unnecessary, but to get an impression of the living chain CLD beyond L. We use the form

$$\ln(R_n) = a\{\ln(n)\}^2 + b\{\ln(n)\} + c \quad (33)$$

where we obtain the coefficients from the values of R_n and the first derivative $d\{\ln(R_n)\}/d\{\ln(n)\}$ at L, together with the requirement that $\sum_{n=1}^{\infty} nR_n = \lambda_1^h$, which quantity is obtained as described above.

The resulting dead and living CLDs are shown in Figure 15 for various k_{db}. The extrapolated living CLDs turn out to be significant in the n^2R_n vs n plot as compared to n^2P_n, although one might expect the CLD at the highest k_{db} to be shifted to higher chain length.

Comparison to Cases with TDB Production by Transfer to Monomer Only. It has been explained before that terminal double bonds are mostly considered to be created by transfer to monomer, but the disproportionation reaction is a possible TDB source as well. In the case of TDBs created by the first mechanism only

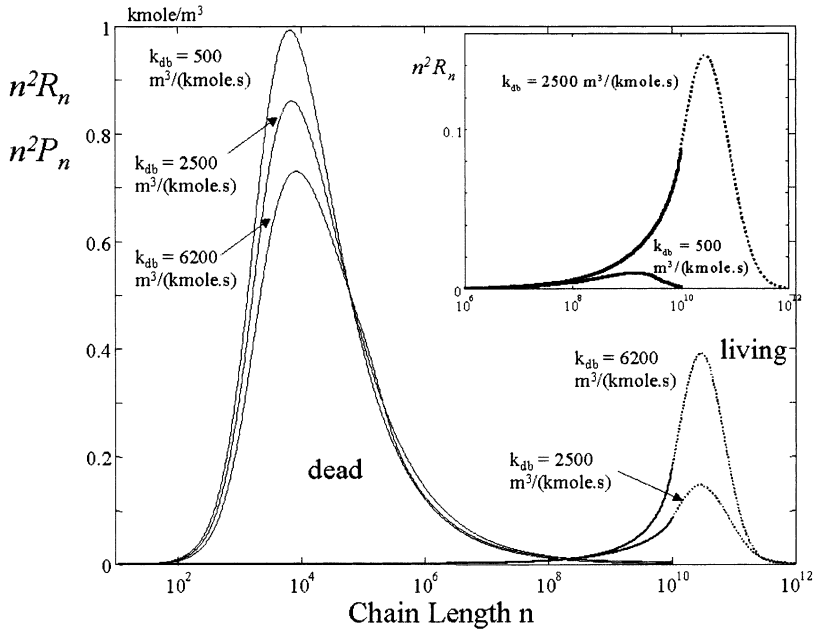

Figure 15. Length distributions of dead and living chains from higher TDB moment distribution model for various TDB propagation rates. Cutoff limit was observed at $L = 10^{10}$. Living CLD complete for $k_{db} = 500$ m^3/(kmol·s) (see inset), for higher k_{db} extrapolation beyond L (dotted curve). Fraction monomer units in living chains in Figure 4.

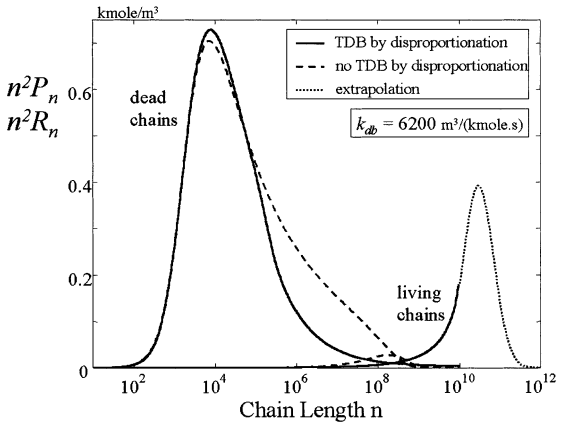

Figure 16. Comparison of dead and living CLDs for the cases of terminal double bonds created by transfer to monomer only (maximum one TDB per chain) and by both transfer to monomer and termination by disproportionation (more than one TDB per chain). $k_{db} = 6200$ m^3/(kmol·s).

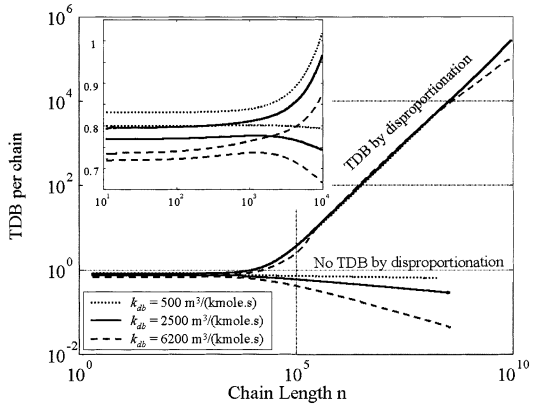

Figure 17. Comparison of TDB distribution $\Psi_n^{1,0}/P_n$ for the cases of terminal double bonds created by transfer to monomer only (maximum one TDB per chain) and by both transfer to monomer and termination by disproportionation (more than one TDB per chain) for various k_{db} (corresponding to CLDs of Figure 16). The plateau region at low n is higher for lower k_{db} (see inset).

and in absence of termination by recombination, chains may carry one TDB at maximum. Here, we compare the present results for the situation of TDBs produced by disproportionation to the previous case of a maximum one TDB per chain. The chain length distributions for the two cases and high TDB propagation rate are depicted in Figure 16. Only for the lowest rate $k_{db} =$ 500 m^3/(kmol·s) is the program able to compute living CLDs completely, without using a cutoff limit (see Supporting Information). It reveals that the CLDs are quite similar for dead chains, while a clear difference exists for the living chains. For the higher TDB propagation rates the dead CLDs become quite different as well. Most interestingly, for the maximum one TDB per chain case, the CLD features a shoulder that becomes higher with increasing k_{db}. This shoulder is absent in the other case, which can be explained by realizing that here the longer chains become more reactive with length because of the higher number of TDBs on longer chains (see Figure 17). Since these chains are more reactive they will be consumed by the TDB propagation reaction more intensively, thereby producing more living chains, as consistent with our findings (see Figure 16). Note that the deviation in the dead CLDs starts at a length of 10^4, at which length also the number of TDBs per chain becomes different. The CLDs for the TDB by disproportionation case do feature a longer tail, which in the n^2P_n vs n plot of Figure 16 even extend beyond the cutoff limit of 10^{10} for the higher k_{db} situations. This renders them an even higher polydispersity. As noted before, the most important portion of monomer units existing in nonmodeled parts of the CLD beyond the cutoff limit is present in living chains. As a general conclusion concerning the CLDs compared here, we observe that the dead CLDs are apparently narrower (no shoulder) in the case of more than one TDB per chain (more reactive dead chains), possess longer tails and contain a comparatively smaller fraction of the monomer units polymerized. When extending the trend

of increasing TDB propagation rate, we would expect a transition to a situation with vanishing dead chain concentrations, while retaining very few but extremely long living chains. Thus, we observe the effect of dead chains with many TDBs acting as cross-linkers between living chains. It should be noted that under such conditions our model is not fully representative anymore. The model should at least be extended by allowing living chains with TDBs to be subject to TDB propagation and, consequently, the existence of multiradicals.

Figure 17 shows the numbers of TDBs per chain as a function of chain length for both cases of TDB production. Here, the contrast is very sharp. While in the maximum of one TDB per chain case the average number of TDBs per chain decreases with chain length, in the more than one TDB case it linearly increases with n in the double-logarithmic plot. The latter implies a reduction to a constant TDB "density" , the number of TDBs per monomer unit in a dead chain. As noted before, this results in a linear increase of dead chain reactivity with chain length, similar to the transfer to polymer reaction.

Conclusions

We have constructed a set of 2-dimensional population balance equations describing chain length and number of TDB distributions for the most general case of an arbitrary number of TDBs per living or dead chain. We have performed this in two different ways. The TDB classes approach employs distinct distribution variables for chains with a certain number of TDBs. The TDB moment distribution approach reduces the original 2-dimensional distribution problem to a 1-dimensional one by taking the moments of the TDB distribution. We argued that assuming transfer to monomer, which creates monomer radicals with a TDB, to be the sole TDB producing mechanism leads to a maximum one TDB per chain. Under these conditions the two modeling approaches become identical and turn out to be solvable without closure relation or assumption.

The results from the one TDB per chain simulations are compared as concerns chain length distributions to earlier Monte Carlo simulation work.[9] Although deviations are not strong, our model when applying the same kinetic parameters generates CLDs with longer tails than the older study does, especially at higher conversion. Also, our model showed higher branching levels at high conversion, although the ratio between branches created by TDB propagation and transfer to polymer are in agreement. These differences must be attributed to differences between the modeling approaches. Some elements of both approaches are essentially identical, however, like the interpretation of the TDB insertion rate coefficient, which in both studies is related to the dead chains with TDBs only. Partially as a consequence of this common view, the average fraction of dead chains containing a TDB is equal in both studies. When comparing our simulation results to experimental data for a CSTR, we observe that the predicted weight-average chain lengths are overestimated, a similar result as found before from moment modeling. When applying a factor of 2.5 lower TDB propagation rate, results do agree, but this also holds for the moment variant of our model. At very high conversion moment, models show the second moment to approach infinity, but the full Galerkin model features a maximum in weight-average chain length.

In view of the discussion on the rate of disproportionation termination and the level of branching, we performed simulations in a range of the associated rate constants: disproportionation and transfer to polymer and TDB insertion, respectively. When in agreement to several earlier studies[6−11] we assume termination to be transfer dominated and consequently to assume a low disproportionation rate, we find high average chain lengths and extremely broad and sometimes bimodal distributions. Also, at long chain lengths, macroradical concentrations exceeding dead chain concentrations were observed. These phenomena exist even without TDB propagation but are indeed enhanced by this mechanism. The occurrence of such relatively high macroradical concentrations has not been shown before. Another important aspect is concerned with chain length distribution modeling in gelling systems, which we now are able to perform, since convergence could be achieved in reasonable computation times. Our model now covers chain length regions well within the gel regime. In combination with experimental data on gel weight fractions and solubility as a function of chain length, we should be able to characterize gels in terms of chain length distribution.

In contrast to the one TDB case, where TDB moment and classes models are mathematically equivalent, for arbitrary TDB numbers per chain they lead to quite different results. This turned out to be so, since the classes model for practical reasons (requiring hundreds of equations) went up to counting only seven TDBs per chain at maximum. This failed to correctly describe the CLD of living and dead chains at greater lengths having much more TDBs, as turned out to be the case from the TDB moment distribution model. The latter revealed the existence of a TDB density—the fraction of monomer units polymerized having a TDB—being constant at longer lengths being at a level of around 5×10^{-5} TDB per monomer unit. In this respect the TDB propagation mechanisms turned out to possess an interesting similarity to the transfer to polymer mechanism, namely the reactivity of dead chains being proportional to their length. Thus, the longest lengths, especially of the living chains, going up to 10^{10} typically contain tens of thousands of TDBs, which is clearly far from the situation as described with the classes model. Consequently, marked differences between the CLDs predicted by both models were observed. The classes model shows relatively high concentrations dead chains at intermediate length, while the moment distribution model predicts much lower values because of their much higher reactivity to TDB propagation. Interestingly, the TDB moment distribution model reveals longer tails for the dead CLD and significantly higher concentrations of extremely long living chains. The effect of highly reactive dead chains with many TDBs acting as cross-linkers indeed turned out to be strong. We observed that higher TDB propagation rates yield increasing fractions of monomer polymerized in living chains—a realistic value for the rate coefficient k_{db} of 6200 $m^3/(kmol \cdot s)$ already resulted in such a fraction of nearly 20%. All of these results only could be obtained by utilizing a concept introduced by us before: the cutoff limit, which here was taken as 10^{10}. Fortunately, all the moments employed in the population balance equations did not require correction terms, as was indeed the case in our previous study, where we had to put the cutoff limit at 10^6. The reason for this circumstance is the fact that

the concentration of living chains $>10^{10}$ is larger by orders of magnitude than that of the dead chains. This implies that the significant part of the monomer units present in nonmodeled parts of CLDs is present in living chains only.

Although the TDB classes model is not correct in view of the limited number of TDBs per chain, the TDB moment distribution model is not exact either. This is because of the higher TDB moment closure problem, for which certain assumptions concerning the polydispersity of the TDB moment distributions have to be made. We have tried moment closures in the models at two levels and compared the results. Implementing a closure relationship obtained from the higher level model into the lower level model gave exactly the same results, so consistency between the models is warranted. The closure relation for the higher moment model was obtained from the TDB classes model, which indicated practical monodispersity for the higher moments. Although this is not a proof, the CLD and TDB distribution results did not turn out to be very sensitive for the assumptions made in this respect. Therefore, we consider the results obtained as sufficiently reliable.

Limitations of the modeling approach of our present study encountered are especially concerned with the neglected reactivity of living chains with many TDBs for TDB propagation. At lower chain lengths living chain concentrations are much lower than dead chain concentrations. However, in the chain length region of interest—here, the concentration of all the chains is low, but in view of their large lengths they may contain a significant number of monomer units—concentrations of dead and living chains are in the same range. In this range, the reactivity of living chains for TDB propagation should be accounted for. This implies that multiradicals have to be dealt with, which is a challenge for further study of this topic.

Supporting Information Available: Text and figures giving model results for the case of a maximum one TDB per chain (effect on CLD and TDB distribution of TDB propagation rate and conversion, which is is illustrated by a number of figures that show that stronger TDB propagation leads to broadening of the CLD and lower values of the fraction chains with TDB), model results for the case of more than one TDB per chain (incorporation of monomer in dead and living chains, illustrated by a figure depicting the fraction of monomer leaving the CSTR as a part of the living chains; a figure showing the comparison between polydispersity D_n from moment and classes model; a comparison of lower and higher TDB moment models, with a figure showing the polydispersity D_n as calculated from the higher TDB moment distribution model (with $D'_n = 1$), and chain length and TDB distributions calculated from lower TDB moment distribution model with two different closure relationships for $\Psi_n^{2.0}$ from $D_n = 1$ and D_n for higher TDB moment distribution model shown by two figures; fraction monomer units in living/dead chain beyond cutoff limit, with two figures showing the living and dead chain concentrations and the fractions beyond the cutoff limit; comparison between cases with TDB production by transfer to monomer only and by disproportionation where Figure 16 of the main text shows results for high TDB insertion rate, but here two figures show the results for lower values; more than one TDB per chain by recombination termination, with results shown in two figures, where the effect of this mechanism on the CLDs turns out to be very strong), and an Appendix giving the derivation of moment model for the case of a maximum one TDB per chain. This material is available free of charge via the Internet at http://pubs.acs.org.

References and Notes

(1) Zhu, S.; Hamielec, A. E. *J. Polym. Sci., Part B: Polym. Phys.* **1994**, *32*, 929−943.
(2) Iedema, P. D.; Hoefsloot, H. C. J. *Macromol. Theory Simul.* **2002**, *11*, 410−428.
(3) Bick, D. K.; McLeish, T. C. B. *Phys. Rev. Lett.* **1996**, *76*, 14, 2587−2590.
(4) Iedema, P. D.; Hoefsloot, H. C. J. *Macromol. Theory Simul.* **2001**, *10*, 855−869.
(5) Iedema, P. D.; Hoefsloot, H. C. J. *Macromol. Theory Simul.* **2001**, *10*, 870−880.
(6) Tobita, H.; Hatanaka, K. *J. Polym. Sci., Part B: Polym. Phys.* **1996**, Vol. *34*, 671−681.
(7) Tobita, H. *Polymer* **1997**, *38*, 1705−1717.
(8) Tobita, H. *J. Polym. Sci., Part B: Polym. Phys.* **1994**, *32*, 901−910.
(9) Tobita, H. *J. Polym. Sci., Part B: Polym. Phys.* **1994**, *32*, 911−919.
(10) Tobita, H.; Hatanaka, K. *J. Polym. Sci., Part B: Polym. Phys.* **1996**, *34*, 671−678.
(11) Chatterjee, A.; Kabra, K.; Graessly, W. W. *J. Appl. Polym. Sci.* **1977**, *21*, 1751−1762.
(12) Nagasubramanian, K.; Graessley, W. W. *Chem. Eng. Sci.* **1970**, *25*, 1549−1558.
(13) Nagasubramanian, K.; Graessley, W. W. *Chem. Eng. Sci.* **1970**, *25*, 1559−1569.
(14) Adelman, R. L.; Ferguson, R. C. *J. Polym. Sci.: Polym. Chem.* **1975**, *13*, 891−911.
(15) Wheeler, L.; Ernst, S. L.; Crozier, R. N. *J. Polym. Sci.* **1952**, *8*, 409−423.
(16) Nozakura, S.-I.; Morishima, Y.; Murahashi, S. *J. Polym. Sci.: Polym. Chem.* **1972**, *10*, 2853−2866.
(17) Hyun, J. C.; Graessly, W. W.; Bankoff, S. G. *Chem. Eng. Sci.* **1976**, *31*, 945−952.
(18) McKenna, T. F.; Villanueva, A. *J. Polym. Sci.: Part A: Polym. Chem.* **1999**, *37*, 589−601.
(19) Britton, D.; Heatley, F.; Lovell, P. A. *Macromolecules* **1998**, *31*, 2828−2837.
(20) Hutchinson, R. A.; Paquet, D. A., Jr.; McMinn, J. H.; Beuermann, S.; Fuller, R.; Jackson, C. *5th International Workshop on Polymer Reaction Engineering*; DECHEMA Monograph 131; VCH Publishers: New York, 1995, p 467.
(21) Pladis, P.; Kiparissides, C. *Chem. Eng. Sci.* **1998**, *53*, 3315−3333.
(22) Iedema, P. D.; Wulkow, M.; Hoefsloot, H. C. J. *Macromolecules* **2000**, *33*, 7173.
(23) Hutchinson, R. A. *Macromol. Theory Simul.* **2001**, *10*, 144.
(24) Wulkow, M. *Macromol. Theory Simul.* **1996**, *5*, 393−416.
(25) Hulburt, H. M.; Katz, S. *Chem. Eng. Sci.* **1964**, *19*, 555−574.
(26) Beuermann, S.; Buback, M.; Nelke, D. *Macromolecules* **2001**, *34*, 6637−6640.
(27) Tobita, H. *J. Polym. Sci., Part B: Polym. Phys.* **2001**, *39*, 391.
(28) Kuchanov, S. I.; Pis'men, L. M. *Polym. Sci. USSR* **1971**, *13*, 2288.

MA020900V